Developmental Biology 350 (2011) 496–510

Contents lists available at ScienceDirect

Developmental Biology

journal homepage: www.elsevier.com/developmentalbiology

Fgf15-mediated control of neurogenic and proneural gene expression regulates dorsal midbrain neurogenesis

Thomas Fischer [a], Theresa Faus-Kessler [a], Gerhard Welzl [a], Antonio Simeone [b], Wolfgang Wurst [a,c,d,*], Nilima Prakash [a,*]

[a] Institute of Developmental Genetics, Helmholtz Centre Munich, German Research Centre for Environmental Health (GmbH), and Technical University Munich, Ingolstaedter Landstr. 1, 85764 Neuherberg, Germany
[b] CEINGE Biotecnologie Avanzate, SEMM European School of Molecular Medicine, and Institute of Genetics and Biophysics "A. Buzzati-Traverso", CNR, Via P. Castellino 111, 80131 Naples, Italy
[c] Max-Planck-Institute of Psychiatry, Kraepelinstr. 2, 80804 Munich, Germany
[d] Deutsches Zentrum für Neurodegenerative Erkrankungen (DZNE) Standort München, Schillerstr. 44, 80336 Munich, Germany

ARTICLE INFO

Article history:
Received for publication 31 August 2010
Revised 14 November 2010
Accepted 13 December 2010
Available online 21 December 2010

Keywords:
Id1/3
Hes5
Neurog1/2
Cell cycle exit
Neural progenitors
Mouse

ABSTRACT

The balanced proliferation and cell cycle exit of neural progenitors, by generating the appropriate amount of postmitotic progeny at the correct time and in the proper location, is required for the establishment of the highly ordered structure of the adult brain. Little is known about the extrinsic signals regulating these processes, particularly in the midbrain. Fibroblast growth factor (Fgf) 15, the mouse ortholog of FGF19 and member of an atypical Fgf subfamily, is prominently expressed in the dorsolateral midbrain of the midgestational mouse embryo. In the absence of *Fgf15*, dorsal midbrain neural progenitors fail to exit the cell cycle and to generate the proper amount of postmitotic neurons. We show here that this is due to the altered expression of inhibitory/neurogenic and proneural/neuronal differentiation helix-loop-helix transcription factor (TF) genes. The expression of *Id1*, *Id3*, and *Hes5* was strongly increased and ectopically expanded, whereas the expression of *Ascl1* (*Mash1*), *Neurog1* (*Ngn1*) and *Neurog2* (*Ngn2*) was strongly decreased and transcription of *Neurod1* (*NeuroD*) was completely abolished in the dorsolateral midbrain of $Fgf15^{-/-}$ mice. These abnormalities were not caused by the mis-expression of cell cycle regulatory proteins such as cyclin-dependent kinase inhibitors or retinoblastoma proteins. Furthermore, human FGF19 promotes cell cycle exit of murine dorsal neural progenitors *in vitro*. Therefore, our data suggest that Fgf15 is a crucial signaling molecule regulating the postmitotic transition of dorsal neural progenitors and thus the initiation and proper progression of dorsal midbrain neurogenesis in the mouse, by controlling the expression of neurogenic and proneural TFs.

Introduction

The establishment of the complex and highly ordered structure of the adult mammalian brain also requires a precisely orchestrated interplay of extrinsic and intrinsic signals during development, that regulate the spatial and temporal balance between self-renewal and cell cycle exit of neural progenitors and the generation of the appropriate numbers of postmitotic progeny. Among the intrinsic signals are TFs of the helix–loop–helix (HLH) family, playing a particularly prominent role in the control of progenitor proliferation, cell cycle exit and neuronal differentiation (Guillemot, 2007). These TFs are therefore classified in three groups: Proneural TFs (Ascl1 (Mash1) and Neurogenins (Neurog, Ngn)) promote the cell cycle exit of neural progenitors and initiation of neurogenesis, and the activation of Notch signaling in adjacent progenitors. Neuronal differentiation TFs (Neurod1 (NeuroD)) are induced by the proneural TFs in postmitotic cells and control the neuronal differentiation program. Inhibitory or neurogenic TFs (Id and Hes) directly inhibit proneural TFs or repress proneural gene expression, thereby maintaining the proliferative, undifferentiated state of neural progenitors. Cell cycle proteins, such as the cyclin-dependent kinase inhibitor (cdki) Cdkn1b ($p27^{Kip1}$) and the retinoblastoma (Rb) proteins Rb1, Rbl1 (p107) and Rbl2 (p130), are another type of intrinsic factors promoting cell cycle exit and differentiation of neural progenitors (Galderisi et al., 2003; Nguyen et al., 2006).

In contrast to the intrinsic factors, the extrinsic signals acting upstream of these TFs or cell cycle proteins are not yet fully established, particularly in the murine midbrain. These are mostly secreted factors, such as bone morphogenetic protein (BMP)/transforming growth factor β (Tgfβ) family members promoting cell cycle exit of neural progenitors (Roussa

* Corresponding authors. Prakash is to be contacted at Institute of Developmental Genetics, Helmholtz Centre Munich, German Research Centre for Environmental Health (GmbH), and Technical University Munich, Ingolstaedter Landstr. 1, 85764 Neuherberg, Germany. Fax: +49 89 3187 3099.
E-mail addresses: wurst@helmholtz-muenchen.de (W. Wurst), nilima.prakash@helmholtz-muenchen.de (N. Prakash).

0012-1606/$ – see front matter © 2010 Elsevier Inc. All rights reserved.
doi:10.1016/j.ydbio.2010.12.017

et al., 2006; Siegenthaler and Miller, 2005); Wnt family members maintaining the proliferative state of neural progenitors, repressing their differentiation, or promoting neurogenesis and neuronal fate specification in a time- and context-dependent manner (Hirabayashi et al., 2004; Kuwabara et al., 2009; Megason and McMahon, 2002; Wexler et al., 2009); and members of the fibroblast growth factor (Fgf) family, which so far have been mostly implicated in the maintenance of the proliferative neural progenitor state (Mason, 2007).

The Fgf family comprises 22 members in mammals, classified in seven subfamilies (Itoh and Ornitz, 2008; Mason, 2007). Fgf15/19, Fgf21 and Fgf23 constitute an atypical Fgf subfamily based on their evolutionary relationship and on the facts that these Fgfs are transcriptionally regulated by members of the nuclear receptor class of ligand activated TFs, possess low-affinity heparin-binding sites and therefore act in an endocrine manner, and require Klotho/β-Klotho transmembrane proteins for efficient signaling via Fgf receptors (Itoh and Ornitz, 2008; Jones, 2008). Mouse Fgf15, despite its low amino acid identity (between 32% and 51%), is considered the structural and functional ortholog of human, chick and zebrafish FGF19/Fgf19 (Miyake et al., 2005; Nishimura et al., 1999; Wright et al., 2004). *Fgf15* expression is confined mostly to the developing central nervous system (CNS) (Gimeno et al., 2003; Ishibashi and McMahon, 2002; McWhirter et al., 1997), but its function was first described in non-neural tissues, where it controls bile acid homeostasis, gall bladder filling and proper morphogenesis of the cardiac outflow tract (Choi et al., 2006; Inagaki et al., 2005; Vincentz et al., 2005). However, a recent report indicated that Fgf15 suppresses proliferation and promotes neural differentiation during neocortical development, although the mechanism of this proneural activity of Fgf15 remained unclear (Borello et al., 2008). Here we show that extrinsic Fgf15 is a crucial signaling molecule regulating the expression of intrinsic inhibitory/neurogenic and proneural HLH TFs in the mouse midbrain, thereby controlling the cell cycle exit of dorsal neural progenitors and their differentiation into neurons.

Materials and methods

Mouse strains

CD-1 mice were purchased from Charles River (Kisslegg/Germany). Generation and genotyping of *Fgf15*$^{+/-}$ mice in a mixed C57BL/6-129/Sv background was described by Wright et al. (2004). These mice were outcrossed with CD-1 mice for 12 generations (F12). *Fgf15*$^{-/-}$ embryos were analyzed from F1 onwards and phenotypic differences were not detected between F1 and F12 embryos. Collection of embryonic stages was done from timed-pregnant females of heterozygous (*Fgf15*$^{+/-}$) intercrosses, noon of the day of vaginal plug detection was designated as embryonic day 0.5 (E0.5). Embryos were additionally staged according to Theiler (1989). Mutant embryos were always compared to their wild-type (*Fgf15*$^{+/+}$) littermates and at least 3 embryos were analyzed for each probe, genotype and stage, if not otherwise indicated in the text. Animal treatment was conducted under federal guidelines and was approved by the HMGU Institutional Animal Care and Use Committee.

Radioactive in situ hybridization (ISH)

Paraffin sections (8 μm) were processed for radioactive ([α-^{35}S]UTP, Amersham/UK) ISH as described in Fischer et al. (2007). Riboprobes used were *Fgf15* (McWhirter et al., 1997), *Fgf8*, *Shh*, *Pax6* and *En1* (Puelles et al., 2003), *Wnt1* (Fischer et al., 2007), *Wnt3a* (Parr et al., 1993), *Id1* (Benezra et al., 1990), *Id3* (Christy et al., 1991), *Hes5* (Akazawa et al., 1992), *Hes3* (Hirata et al., 2001), *Ascl1* (*Mash1*), *Neurog1* (*Ngn1*), *Neurog2* (*Ngn2*) and *Neurod1* (*NeuroD*) (Cau et al., 1997; Ma et al., 1997), Helt (Mgn) (Guimera et al., 2006a), *Dll1* (Bettenhausen et al., 1995), *Dusp6* (*Mkp3*) (Echevarria et al., 2005), *Fgfr1-3* (Blak et al., 2005), *Spry2* (Minowada et al., 1999), *Etv4* (*Pea3*) and *Etv5* (*Erm*) (Blak et al., 2007). Images were taken with an Axioplan2 microscope or StemiSV6 stereomicroscope using bright- and dark-field optics, AxioCam MRc camera and Axiovision 4.6 software (Zeiss/Germany), and processed with Adobe Photoshop 7.0 or CS software (Adobe Systems Inc./USA).

Immunohistochemistry (IHC)

Antigens were detected on paraffin (8 μm) or cryosections (16 μm) as reported by Brodski et al. (2003) and Puelles et al. (2004). Primary monoclonal antibodies used were mouse anti- 5-bromo-2′-deoxyuridine (BrdU) (1:10; Roche Diagnostics/Germany) and βIII-Tubulin (Tubb3, TuJ1) (1:5000; Chemicon/USA), and rat anti-Nestin (1:3; BD Pharmingen/USA). Polyclonal antisera used were rabbit anti-cleaved Caspase 3 (cCasp3) (1:200; Cell Signaling/USA), phosphorylated Histone H3 (pH3) (1:1000; Upstate/USA), Ki-67 (1:100; Vision BioSystems/UK) and Doublecortin (Dcx) (1:80, gift from O. Reiner, Weizmann Institute of Science/Israel). Secondary antibodies were either fluorescently labelled (Cy3/Cy2) or coupled to biotin/streptavidin-horseradish-peroxidase (Jackson ImmunoResearch Laboratories/USA), and detected using the VECTOR® M.O.M.™ and Vectastain ABC System (Vector Laboratories/USA). Fluorescent images were taken with an Axiovert 200 M inverted microscope (Zeiss) and processed with Adobe Photoshop 7.0 or CS software.

BrdU treatments

Intraperitoneal (i.p.) injections of pregnant dams with 31 μg BrdU (Sigma/Germany)/g body weight were performed on E11.5 for single (10 min) or cumulative (3× every 2 hours (hrs)) labeling. Embryos were dissected 10 min (single labeling) or 2 hrs (cumulative labeling) after the last injection and processed for immunodetection of BrdU.

Cell countings

Ki67$^+$ and pH3$^+$ cells were counted on serial coronal sections from E11.5 embryos using the Neurolucida 6 software (MBF Bioscience/USA). Cell numbers were averaged for each genotype and subjected to tests for the estimation of statistical significance as described in Statistical analyses.

Cell cycle exit assay

Pregnant dams from *Fgf15*$^{+/-}$ intercrosses were injected i.p. with BrdU (31 μg/g body weight) on E10.5 (t_0). Embryos were dissected 24 hrs later (t_{24}) at E11.5 and processed for fluorescent immunodetection of BrdU and Ki-67. Stained sections were evaluated with a confocal laser scanning microscope (LSM 510 META, Zeiss). A *z*-stack image series in intervals of 1 μm was recorded from each section comprising the entire thickness of the tissue. The index T_c of cell cycle re-entry after 24 hrs was calculated by dividing the number of Ki-67$^+$/BrdU$^+$ double-labeled cells by the total number of BrdU$^+$ cells.

Immunoblotting

The anterior neural tube (fore-/midbrain and rhombomere 1) of E11.5 embryos from *Fgf15*$^{+/-}$ intercrosses was dissected free of non-neural tissues and eye cups in ice-cold tissue lysis buffer (20 mM Tris pH7.5, 150 mM NaCl, 1 mM EDTA, 1 mM EGTA, 1% Triton X-100, protease and phosphatase inhibitors (complete Mini and PhosSTOP, Roche)) and homogenized in 100 μl tissue lysis buffer. The remaining embryonic tissue was used for PCR genotyping. Total protein content was determined by Bradford assay (Sigma-Aldrich/Germany). Equal amounts of total protein from tissue lysates were separated in 4–12% Criterion XT Bis-Tris Precast gels (Bio-Rad/Germany) together with controls and a biotinylated protein ladder following the manufacturer's instructions (PhosphoPlus Rb antibody kit, Cell Signaling), and blotted onto nitrocellulose membranes (Hybond-ECL, GE Healthcare Europe/

Germany). Blots were probed with rabbit anti-phosphorylated RB1 (Ser807/811) (1:1000; Cell Signaling) and anti-RBL1 (p107) (1:2000; Santa Cruz Biotechnology/USA); and mouse anti-Cdkn1b ($p27^{Kip1}$) (1:2500; BD Pharmingen), anti-RB1 (p110) (1:500; BD Pharmingen) and anti-active (dephosphorylated) β-Catenin (1:1000; Upstate) antibodies. Membranes were stripped in 0.2 M Glycine-HCl pH2.5, 0.1% Tween-20, and reprobed with mouse anti-β-Actin antibody (1:5000; Abcam/UK) as a loading control. Densitometric analysis of the immunoblots was performed with a GS-800 Calibrated Densitometer (Bio-Rad) and ImageJ 1.34 s software (NIH/USA). Variations in total protein content were corrected within each blot by using the amount of β-Actin protein as standard.

Primary cell cultures and clonal analyses

Primary cortical progenitor cell cultures were prepared from E12.5 CD-1 embryos as described in Hartfuss et al. (2001). Cells were plated at a density of 800,000 cells/well on poly-D-lysine coated coverslips and infected with a green fluorescent protein (GFP)-expressing retrovirus 2 hrs after plating as reported by Malatesta et al. (2000). Three hours after retroviral infection and with each medium change, recombinant human FGF19 protein (R&D Systems/USA) was added to a final concentration of 5 ng/ml. After 7 days in culture, cells were fixed and processed for immunocytochemical detection of GFP and Tubb3 as described in Berninger et al. (2007). GFP^+ cell clones were evaluated with an Axioplan2 microscope/AxioCam HRm camera (Zeiss), and the number of GFP^+ and $GFP^+/Tubb3^+$ double-labeled cells was counted for each clone using Axiovision 4.6 software (Zeiss). The mean was calculated from the total number of clones analyzed with or without FGF19 treatment ± s.e.m. Data were derived from four independent experiments.

Statistical analyses

For analysis of the effect of an experimental factor (genotype or treatment) with data from different brain regions or several independent experiments, two-way ANOVA was applied. First, an ANOVA with interaction between factor and experiment was fitted. If the interaction effect was significant, *t*-tests were performed for the individual experiments. Otherwise a two-way ANOVA without interaction effect was fitted, and post-hoc *t*-tests with *P*-value adjustment according to Holm (1979) were performed. For cell cycle experiments with several sections per embryo, genotypes were compared by one-way ANOVA for repeated measurements. For all calculations, the R software with the nlme package was used (Pinheiro et al., 2008; R Development Core Team, 2009).

Results

Fgf15 is expressed in dorsal regions of the mouse midbrain

We first mapped the expression of *Fgf15* in relation to Fgf8 and Shh, two crucial signaling molecules controlling antero-posterior (A/P) and

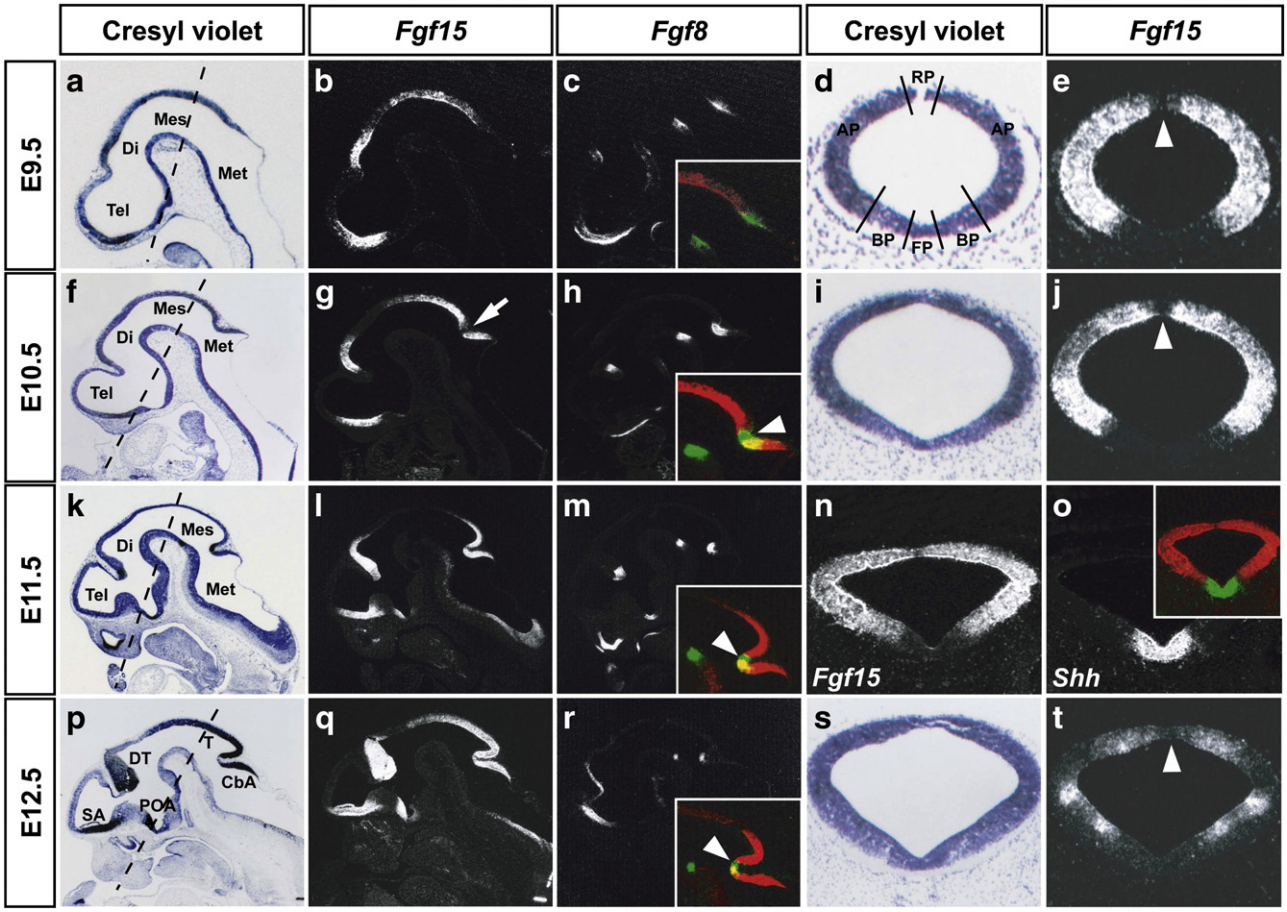

Fig. 1. *Fgf15* is expressed in dorsal regions of the mouse midbrain. (a–t) Representative sagittal (a–c, f–h, k–m, p–r) and coronal midbrain (d, e, i, j, n, o, s, t) sections (anterior left, dorsal top; coronal level indicated by broken lines in a, f, k, p) of wild-type (CD-1) mouse embryos at E9.5 (a–e), E10.5 (f-j), E11.5 (k-o) and E12.5 (p–t). (b, g, l, q, e, j, t) are darkfield views of (a, f, k, p, d, i, s), respectively. Insets in (c, h, m, r, o) are pseudo-colored overlays of consecutive sections hybridized with probes for *Fgf15* (red) and *Fgf8* (green in c, h, m, r) or *Shh* (green in o); overlapping expression domains appear in yellow. *Fgf15* is expressed in the dorsal di-, mes- and metencephalon, with a gap in the rostral $Fgf8^+$ domain at the MHB (white arrow/arrowheads in g and insets in h, m, r), and sparing the RP (white arrowhead in e, j, t) and the Shh^+ BP and FP (inset in o). Abbreviations: AP, alar plate; BP, basal plate; CbA, cerebellar anlage; Di, diencephalon; DT, dorsal thalamus; FP, floor plate; Mes, mesencephalon; Met, metencephalon; POA, preoptic area; RP, roof plate; SA, septal area; T, tectum; Tel, telencephalon.

dorso-ventral (D/V) patterning of the brain (Fig. 1). Between E9.5 and E12.5, *Fgf15* expression was confined mostly to dorsal regions of the di-, mes- and metencephalon and exhibited a decreasing gradient at both sides of the isthmic constriction (Fig. 1). Metencephalic *Fgf15* transcription overlapped with the caudal *Fgf8*$^{+}$ domain, but mesencephalic *Fgf15* expression showed a sharp, non-overlapping border with the rostral *Fgf8*$^{+}$ domain at the mid-/hindbrain boundary (MHB). As the midbrain was one of the most prominent sites of *Fgf15* expression within the neural tube of the midgestational mouse embryo, we focused our analysis on this brain region. From E9.5 to E11.5, *Fgf15* was expressed throughout the neuroepithelium in the dorsal two thirds of the mesencephalon, sparing the roof plate (RP) and abutting the *Shh*$^{+}$ floor (FP) and basal plate (BP) (Fig. 1). Notably, *Fgf15* expression refined to discrete sites at both sides of the RP and of the BP at E12.5, with lowest *Fgf15* transcription in an intermediate zone located approximately at the level of the dorsolateral sulcus of the midbrain (Fig. 1). Thus, *Fgf15* expression is confined to dorsolateral regions of the midgestational mouse midbrain and does not overlap with *Fgf8* and *Shh*.

Embryonic lethality and CNS defects in outbred Fgf15$^{-/-}$ *mice*

The lack of a CNS phenotype in *Fgf15*$^{-/-}$ mice on a mixed C57BL/6-129/Sv and inbred C57BL/6 genetic background (Vincentz et al., 2005; Wright et al., 2004) (our own observations), despite the prominent neural expression of *Fgf15* in the midgestational mouse embryo, prompted us to outcross the *Fgf15*$^{+/-}$ mice into a CD-1 genetic background. The genotype and morphologically abnormal phenotype distribution of embryos obtained from *Fgf15*$^{+/-}$ intercrosses in the first five (F1-F5), tenth (F10) and twelfth (F12) outcross generations are summarized in Supplementary Table 1. In the first and second (F1–F2) outcross generation, the frequency of *Fgf15*$^{-/-}$ embryos recovered at E13.5 or later was much lower than expected by the Mendelian ratios and, in particular, no *Fgf15*$^{-/-}$ mutants were found at E17.5 and E18.5. From the third (F3) outcross generation onwards, *Fgf15*$^{-/-}$ embryos were recovered at approximately Mendelian ratios up to E11.5, indicating that most mutant embryos died after this time-point during development. The outer inspection of the *Fgf15*$^{-/-}$ embryos showed that around 10% of the E11.5 mutants, 20% of the E12.5 mutants, and more than 30% of the E13.5 mutants displayed morphological abnormalities such as a poorly vascularized chorion, pale appearance and a clear growth retardation (Suppl. Table 1 and Fig. 2). Sagittal and coronal sections of these morphologically abnormal mutant embryos revealed a massive overgrowth and infolding of dorsal neural tissues (Fig. 2). Furthermore, apoptotic cell death was dramatically increased in the *Fgf15*$^{-/-}$ embryos displaying an abnormal morphology at E12.5, whereas it did not differ from their wild-type littermates at E11.5 (Suppl. Fig. S1). All the other *Fgf15*$^{-/-}$ embryos were morphologically indistinguishable from their wild-type littermates (Suppl. Table 1). The blood vessels of the perineural vascular plexus had developed normally and were filled with erythrocytes in the E11.5 *Fgf15*$^{-/-}$ embryos (Suppl. Fig. S1), indicating that blood supply of neural tissues was intact in the mutant embryos up to this stage. These results showed that the *Fgf15* null mutation in an outbred (CD-1) genetic background was embryonic lethal after E11.5, and that up to one tenth of the *Fgf15*$^{-/-}$ embryos displayed severe CNS defects already at this stage.

Dorsal neural progenitors fail to exit the cell cycle in Fgf15$^{-/-}$ *embryos*

The massive overgrowth and infolding of dorsal neural tissues in more than one third of the outbred *Fgf15*$^{-/-}$ embryos at E13.5 suggested a more general defect of dorsal neural tube development in the mutant embryos. Since the frequency of morphological CNS defects increased after E11.5 in outbred *Fgf15*$^{-/-}$ embryos, and most of these embryos appeared to die 2 days later, we focused our analyses on morphologically normal *Fgf15*$^{-/-}$ embryos at E11.5. The

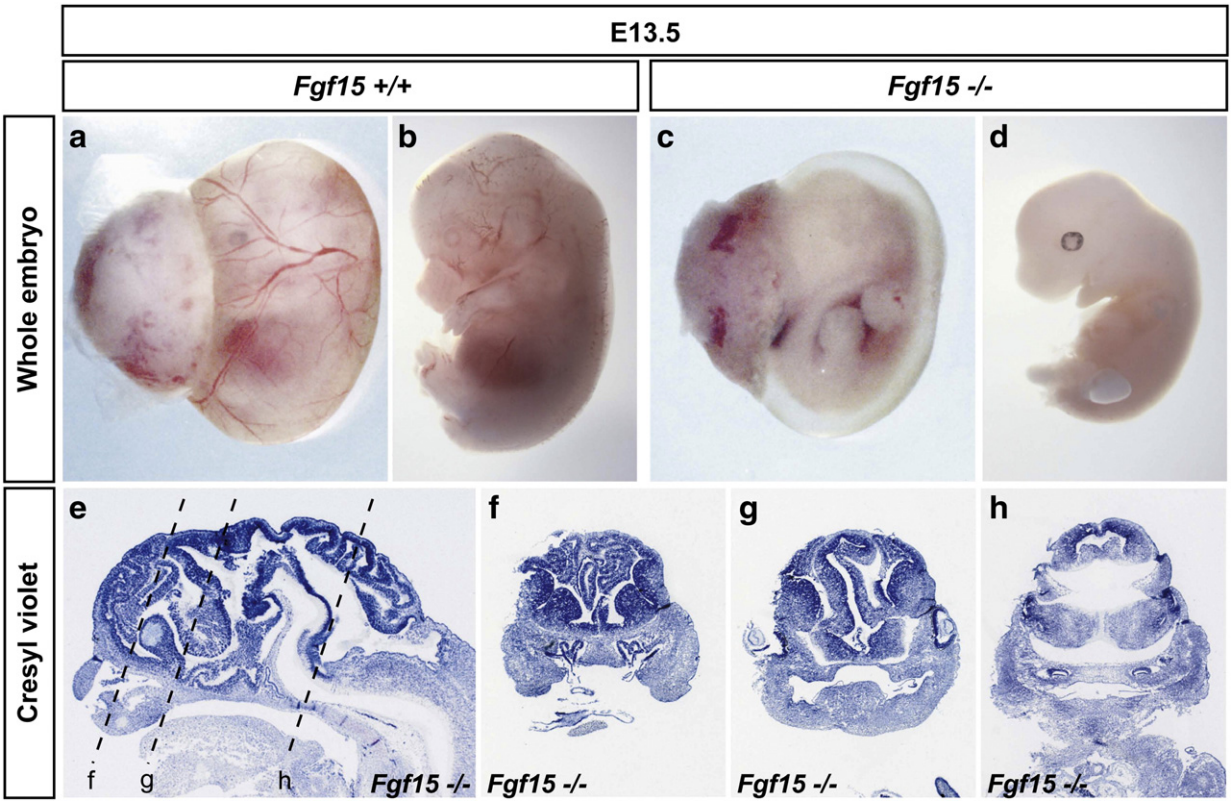

Fig. 2. Morphological and CNS defects in outbred *Fgf15*$^{-/-}$ embryos. (a–d) Representative images of an E13.5 wild-type (*Fgf15*$^{+/+}$) embryo (a, b) and its *Fgf15*$^{-/-}$ littermate (c, d) on an outbred (CD-1) genetic background. More than 30% of the outbred *Fgf15*$^{-/-}$ embryos displayed a poorly vascularized chorion membrane, pale appearance and manifest growth-retardation at this stage. (e–h) Representative sagittal (e) and coronal (f–h) Nissl-stained sections (anterior left, dorsal top; coronal level indicated by broken lines in e) from E13.5 *Fgf15*$^{-/-}$ embryos, showing a massive overgrowth and infolding of dorsal neural tissues in these mutant embryos.

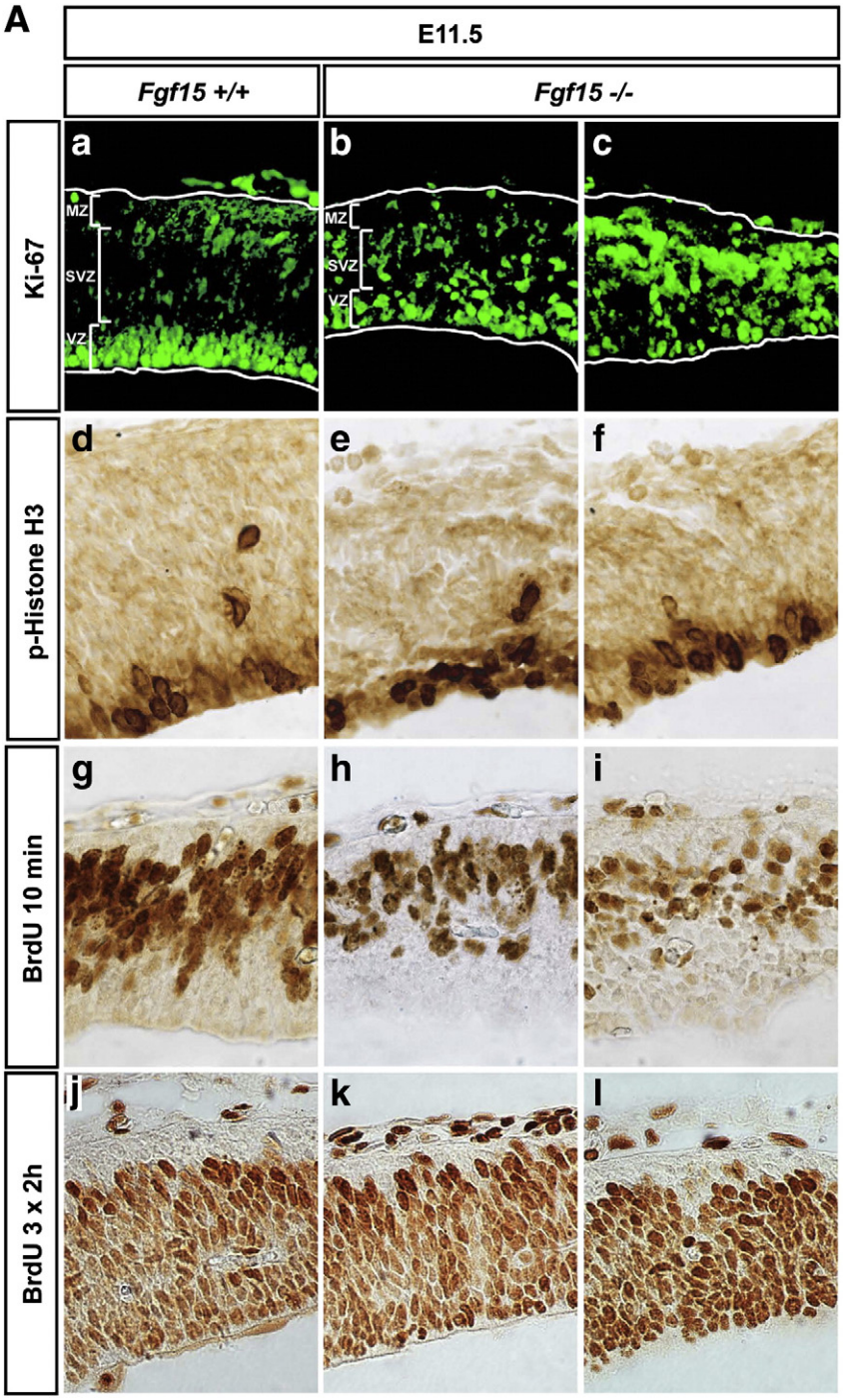
A
E11.5
Fgf15 +/+
Fgf15 -/-
Ki-67
p-Histone H3
BrdU 10 min
BrdU 3 x 2h
a
b
c
d
e
f
g
h
i
j
k
l
MZ
SVZ
VZ
B
Ki-67+ cells by Region in groups of Genotype
means with the 1 fold of the standard error of the mean
Ki-67+ cells/section
Fgf15 +/+
Fgf15 -/-
Forebrain
Midbrain
Hindbrain
Cell density by Region in groups of Genotype
means with the 1 fold of the standard error of the mean
pH3+ cells/area (µm2)
Fgf15 +/+
Fgf15 -/-
Forebrain
Midbrain
Hindbrain

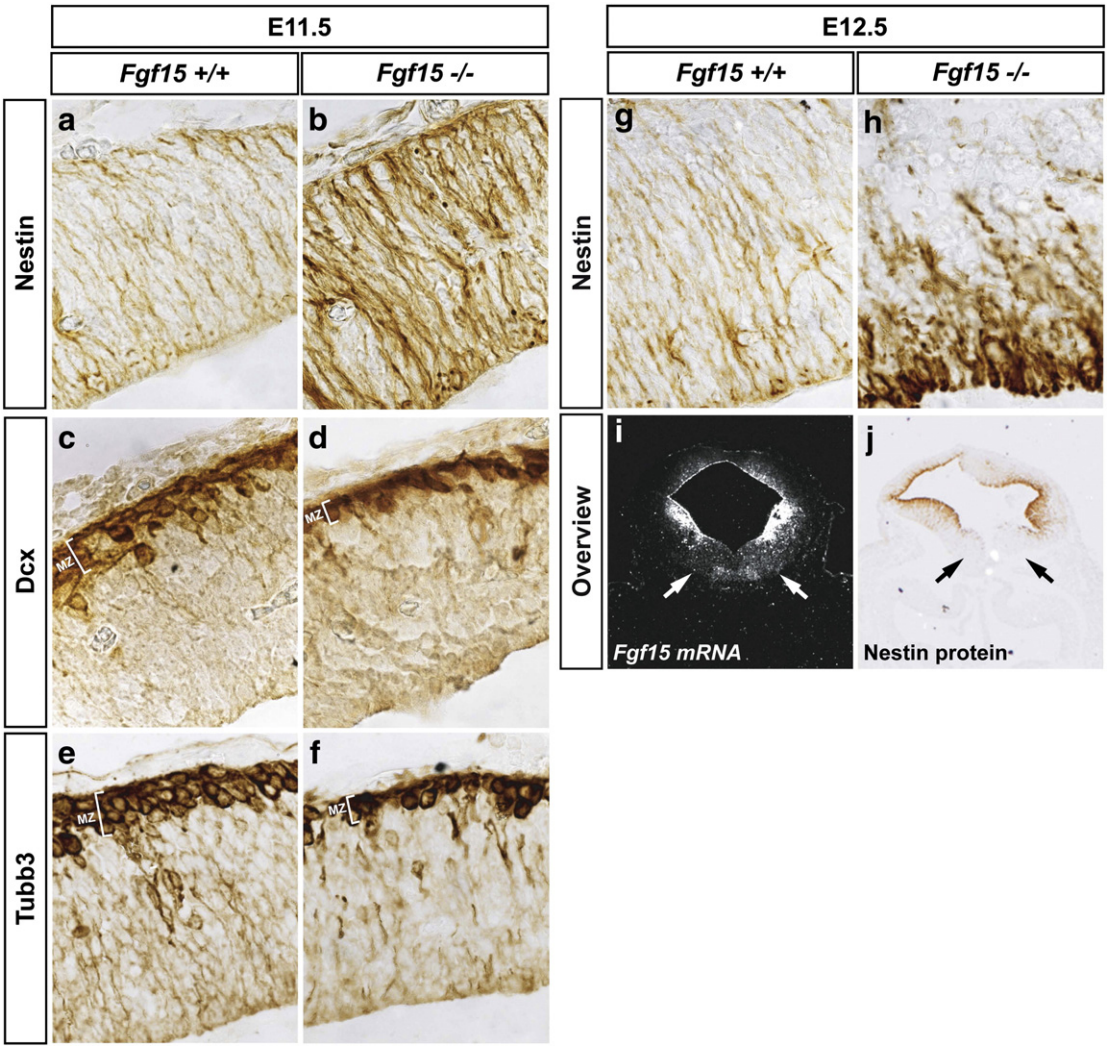

Fig. 4. Increased Nestin expression and reduced amount of Dcx$^+$/Tubb3$^+$ postmitotic neurons in the *Fgf15*$^{-/-}$ dorsolateral midbrain. (a–h) Representative close-up views of the dorsal midbrain (pial surface top) on coronal sections from wild-type (*Fgf15*$^{+/+}$) (a, c, e, g) and *Fgf15*$^{-/-}$ (b, d, f, h) embryos at E11.5 (a–f) and E12.5 (g, h). Nestin expression in the *Fgf15*$^{-/-}$ dorsolateral midbrain was increased at E11.5 (a, b), and appeared distorted at E12.5 (g, h). Postmitotic Dcx$^+$ and Tubb3$^+$ neurons occupied only one cell layer within the mantle zone (MZ) of the mutants, as compared to the 2–3 cell layers in wild-type embryos (white brackets in c–f). (i, j) Representative coronal midbrain sections from wild-type (*Fgf15*$^{+/+}$) (i) and *Fgf15*$^{-/-}$ (j) embryos at E12.5. Nestin expression was strongly increased in the *Fgf15*$^{-/-}$ dorsolateral midbrain (j), where *Fgf15* is highly expressed in the wild-type embryo (i). Nestin was very weakly expressed in the *Fgf15*$^{-/-}$ ventral midbrain at this stage, where *Fgf15* is normally not expressed (arrows in i, j).

expression of *Pax6*, *En1*, *Fgf8*, *Shh*, *Wnt1* and *Wnt3a* was not affected in the mutant embryos (Suppl. Figs. S2 and S3), suggesting that regional identities were properly induced in the absence of *Fgf15*. We noted, however, that all mutants exhibited a thinner dorsal neuroepithelium, and we thus assessed neural progenitor proliferation in these embryos. The total number of proliferating Ki-67$^+$ cells was significantly increased in the *Fgf15*$^{-/-}$ embryos, which in addition were ectopically positioned throughout the dorsal midbrain neuroepithelium, although the numbers and distribution of phospho-Histone H3$^+$ (pH3$^+$) and BrdU$^+$ cells were not severely affected in the mutants (Fig. 3). These data suggested that the number of cycling dorsal neural progenitors was significantly increased in the *Fgf15*$^{-/-}$ embryos.

The thinning of the mutant dorsal neuroepithelium also suggested that despite the increased numbers of cycling progenitors, these cells did not generate the proper numbers of postmitotic progeny. Indeed, Doublecortin$^+$ (Dcx) and βIII-Tubulin$^+$ (Tubb3, TuJ1) postmitotic neurons were remarkably reduced and occupied only 1 cell layer in the mantle zone (MZ) of the mutant dorsal midbrain instead of the 2–3 cell layers detected in wild-type embryos (Fig. 4). By contrast, expression of the intermediate filament Nestin, a marker for neural stem and progenitor cells that is down-regulated as soon as these cells

Fig. 3. Increased numbers of proliferating dorsal neural progenitors in the *Fgf15*$^{-/-}$ embryos. (A) Representative close-up views of the dorsal midbrain (pial surface top) on coronal sections from E11.5 wild-type (*Fgf15*$^{+/+}$) (a, d, g, j) and *Fgf15*$^{-/-}$ (b, c, e, f, h, i, k, l) embryos. The *Fgf15*$^{-/-}$ embryos in (c, f, i, l) displayed a stronger phenotype than the ones shown in (b, e, h, k). Proliferating Ki-67$^+$ cells were increased and ectopically positioned in the *Fgf15*$^{-/-}$ dorsal neuroepithelium (a–c), although the number and distribution of phospho-Histone H3$^+$ (pH3$^+$) and BrdU$^+$ cells was not severely affected in the mutants (d–l). Note the thinner neuroepithelium in the *Fgf15*$^{-/-}$ embryos. (B) Quantification of Ki-67$^+$ and pH3$^+$ cells in wild-type and *Fgf15*$^{-/-}$ embryos. (m) The number of Ki-67$^+$ cells/section was increased from 31.67 ± 1.43 (*Fgf15*$^{+/+}$) to 34.63 ± 1.27 (*Fgf15*$^{-/-}$) in the dorsal forebrain, from 30.89 ± 0.63 (*Fgf15*$^{+/+}$) to 34.36 ± 0.9 (*Fgf15*$^{-/-}$) in the dorsal midbrain, and from 32.0 ± 1.95 (*Fgf15*$^{+/+}$) to 38.13 ± 2.06 (*Fgf15*$^{-/-}$) in the dorsal hindbrain (*Fgf15*$^{+/+}$, n = 3; *Fgf15*$^{-/-}$ *n* = 4; mean ± s.e.m.). This increase was significant in the two-way ANOVA (asterisk, *P* = 0.035). In post-hoc *t*-tests with *P*-value adjustment, there was no significance for any of the brain regions separately. (n) pH3$^+$ cells/1000 μm^2 were increased from 0.77 ± 0.07 (*Fgf15*$^{+/+}$) to 0.87 ± 0.04 (*Fgf15*$^{-/-}$ in the dorsal forebrain, from 0.60 ± 0.03 (*Fgf15*$^{+/+}$) to 0.73 ± 0.04 (*Fgf15*$^{-/-}$ in the dorsal midbrain, and from 0.58 ± 0.02 (*Fgf15*$^{+/+}$) to 0.70 ± 0.05 (*Fgf15*$^{-/-}$) in the dorsal hindbrain (*n* = 4/genotype; mean ± s.e.m.). This increase was not significant (*P* = 0.063 for the genotype effect in the two-way ANOVA). Abbreviations: MZ, mantle zone; SVZ, subventricular zone; VZ, ventricular zone.

become postmitotic (Lendahl et al., 1990), was strongly increased in the dorsal midbrain of E11.5 *Fgf15*$^{-/-}$ embryos (Fig. 4). The aberrant expression of Nestin was even more pronounced in the mutant embryos at E12.5. Immunostaining for Nestin at this stage was strongest and appeared severely distorted in the *Fgf15*$^{-/-}$ dorsolateral midbrain, where *Fgf15* is highly expressed in the midgestational wild-type embryo, whereas it was very weak in the mutant ventral midbrain, where *Fgf15* is normally not expressed (Fig. 4). These results suggested that Fgf15 directly controls the postmitotic transition of dorsal neural progenitors in the midbrain.

The increased numbers and ectopic distribution of Ki-67^{+} proliferating cells, as well as the corresponding reduction of Tubb3^{+} postmitotic neurons, strongly suggested that dorsal neural progenitors failed to exit the cell cycle in the *Fgf15*$^{-/-}$ embryos. Therefore, we injected BrdU into pregnant *Fgf15*$^{+/-}$ females at E10.5, 24 hrs before dissection of the embryos at E11.5. Double-staining for BrdU and Ki-67 should reveal the fraction of BrdU^{+}/Ki67^{+} cells that had re-entered the cell cycle during this 24 hr-period (Fig. 5). Compared to E11.5 control embryos, this fraction was significantly increased by 60% in the dorsal neuroepithelium of the *Fgf15*$^{-/-}$ embryos, whereas the complementary fraction of BrdU^{+}/Ki-67^{-} cells that had exited the cell cycle during the 24 hr-period was significantly decreased by approximately 11% in the mutants (Fig. 5). Moreover, BrdU^{+}/Ki-67^{+} progenitors were ectopically positioned in the SVZ of all mutant embryos analyzed, and even found in the MZ in about 20% of the *Fgf15*$^{-/-}$ embryos (Fig. 5). These data confirmed that dorsal neural progenitors failed to exit the cell cycle and were ectopically located in the mesencephalic neuroepithelium of the outbred *Fgf15*$^{-/-}$ embryos.

Neurogenic/inhibitory genes are upregulated and proneural genes are downregulated in the Fgf15$^{-/-}$ *dorsolateral midbrain*

Dorsal neural progenitors might fail to exit the cell cycle in the *Fgf15*$^{-/-}$ embryos due to the de-regulation of crucial cell cycle proteins, such as cdki or Rb proteins (Galderisi et al., 2003); or due to the misexpression of neurogenic and proneural genes that in turn regulate cell cycle exit and neuronal differentiation (Bertrand et al., 2002). No significant variation in the levels of phosphorylated Rb1

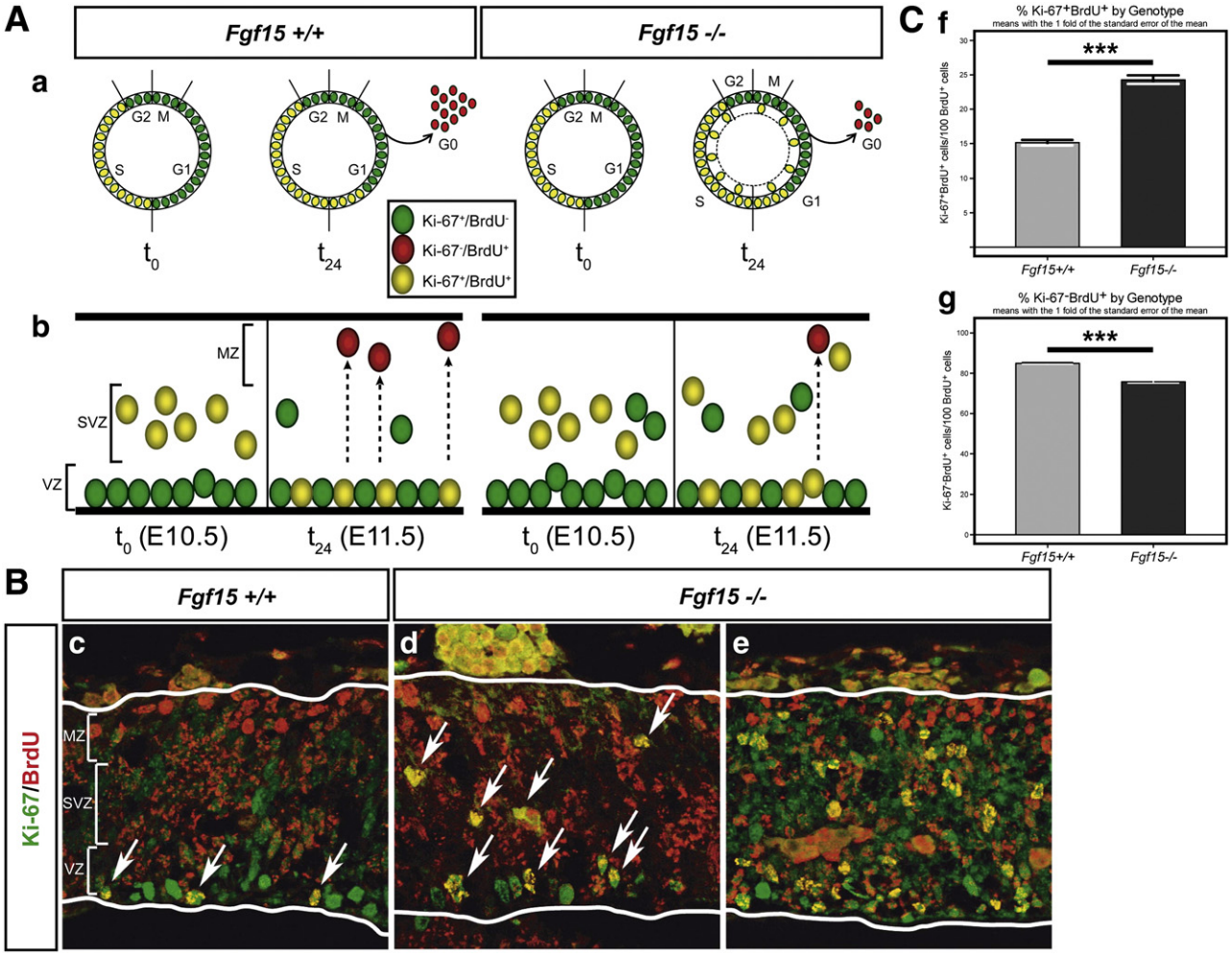

Fig. 5. Dorsal neural progenitors fail to exit the cell cycle and are ectopically positioned in *Fgf15*$^{-/-}$ embryos. (A) Scheme depicting the experimental paradigm. (a) Proliferating neural progenitors express Ki-67 (Ki-67^{+}/BrdU^{-} cells, green ovals). Cells in the S-phase of the cell cycle incorporate BrdU at E10.5 (t_0) (Ki-67^{+}/BrdU^{+} cells, yellow ovals). After 24 hrs (at E11.5; t_{24}), a fraction of the Ki-67^{+}/BrdU^{+} progeny had exited the cell cycle (G_0-phase) and initiated neuronal differentiation (Ki-67^{-}/BrdU^{+} cells, red ovals), while the remaining progeny continued to cycle. A cell cycle exit defect in the mutant embryos leads to an accumulation of Ki-67^{+}/BrdU^{+} proliferating cells and reduction of the Ki-67^{-}/BrdU^{+} G_0 fraction. (b) As neuroepithelial cells exit the cell cycle and become postmitotic (Ki-67^{-}/BrdU^{+}, red), they migrate out of the VZ into the MZ. Ki-67^{+}/BrdU^{-} (green) and Ki-67^{+}/BrdU^{+} (yellow) proliferating progenitors are confined mostly to the VZ in the wild-type (*Fgf15*$^{+/+}$), but are ectopically positioned in the SVZ/MZ of the *Fgf15*$^{-/-}$ embryos. (B) Representative close-up views of the dorsal midbrain (pial surface top) on coronal sections from wild-type (*Fgf15*$^{+/+}$) (c) and *Fgf15*$^{-/-}$ (d, e) embryos at E11.5 (t_{24}), treated with BrdU at E10.5 (t_0). Ki-67^{+} (green)/BrdU^{+} (red) double-labeled cells (in yellow; white arrows in c, d) are increased and ectopically positioned in the mutants. Approximately 20% of the *Fgf15*$^{-/-}$ embryos showed a stronger cell cycle exit defect (e). (C) The index Tc (percentage of Ki-67^{+} and BrdU^{+} cells/total BrdU^{+} cells) of cell cycle re-entry after 24 hrs was significantly increased by 60% in the *Fgf15*$^{-/-}$ embryos (*Fgf15*$^{+/+}$, 15.14 ± 0.41, n = 3; *Fgf15*$^{-/-}$, 24.28 ± 0.61, $n = 4$; mean ± s.e.m.) (f), whereas the percentage of Ki-67^{-} and BrdU^{+} cells/total BrdU^{+} cells that had exited the cell cycle after 24 hrs was significantly reduced by approximately 11% in the *Fgf15*$^{-/-}$ embryos (*Fgf15*$^{+/+}$, 84.86 ± 0.41, $n = 3$; *Fgf15*$^{-/-}$, 75.72 ± 0.61, $n = 4$; mean ± s.e.m.) (g); triple asterisks: $P < 0.0001$ in the one-way repeated-measurements ANOVA. Abbreviations: G_0, G_1, S, G_2, M, phases of the cell cycle; MZ, mantle zone; SVZ, subventricular zone; VZ, ventricular zone.

(the inactive form of Rb1), Rbl1 (p107) and Cdkn1b ($p27^{Kip1}$) was observed in the *Fgf15*$^{-/-}$ anterior neural tube at E11.5 (Suppl. Fig. S4), suggesting that the expression of these cell cycle proteins was not affected by the lack of Fgf15. An increased activation of the Wnt/β-Catenin pathway was previously reported in the *Fgf15*$^{-/-}$ cortex (Borello et al., 2008), and the phenotype of the morphologically abnormal *Fgf15*$^{-/-}$ embryos indeed resembled a mouse mutant over-expressing a constitutively active form of β-Catenin (Chenn and Walsh, 2002). However, the protein levels of the activated (dephosphorylated) form of β-Catenin were not changed between wild-type and *Fgf15*$^{-/-}$ brains at E11.5 (Suppl. Fig. S4).

We then analyzed the expression patterns of different HLH TFs in the *Fgf15*$^{-/-}$ embryos between E9.5 and E11.5. These TFs may be grouped in neurogenic factors sustaining proliferation (*Hes3* and *Hes5*; (Kageyama et al., 2007)), inhibitors of differentiation (*Id1* and *Id3*; (Ruzinova and Benezra, 2003)), or proneural factors promoting cell cycle exit and neuronal differentiation (*Ascl1* (*Mash1*), *Neurog1* (*Ngn1*), *Neurog2* (*Ngn2*) and *Neurod1* (*NeuroD*); (Bertrand et al., 2002)). Remarkably, a strong increase and ectopic expansion of *Hes5* and *Id3* transcription in the ventrolateral and dorsolateral *Fgf15*$^{-/-}$ midbrain was first detected at E10.5, and at E11.5, *Id1*, *Id3* and *Hes5* were strongly up-regulated and ectopically expressed in the mutant dorsal midbrain (Fig. 6). By contrast, the transcription of the proneural bHLH TFs *Ascl1* and *Neurog1* was diminished in the mutant dorsolateral midbrain at E9.5 and E10.5, respectively, (Fig. 7). At E11.5, the expression of *Ascl1*, *Neurog1* and *Neurog2* was heavily reduced, and that of *Neurod1*, acting downstream of Ascl1 and Neurog2 (Guillemot, 2007), was totally silenced in the *Fgf15*$^{-/-}$ dorsolateral midbrain (Fig. 7). These findings indicated that Fgf15 controls the cell cycle exit and differentiation of dorsal midbrain neural progenitors by suppressing the expression of neurogenic and inhibitory Hes5 and Id3, and/or by activating the

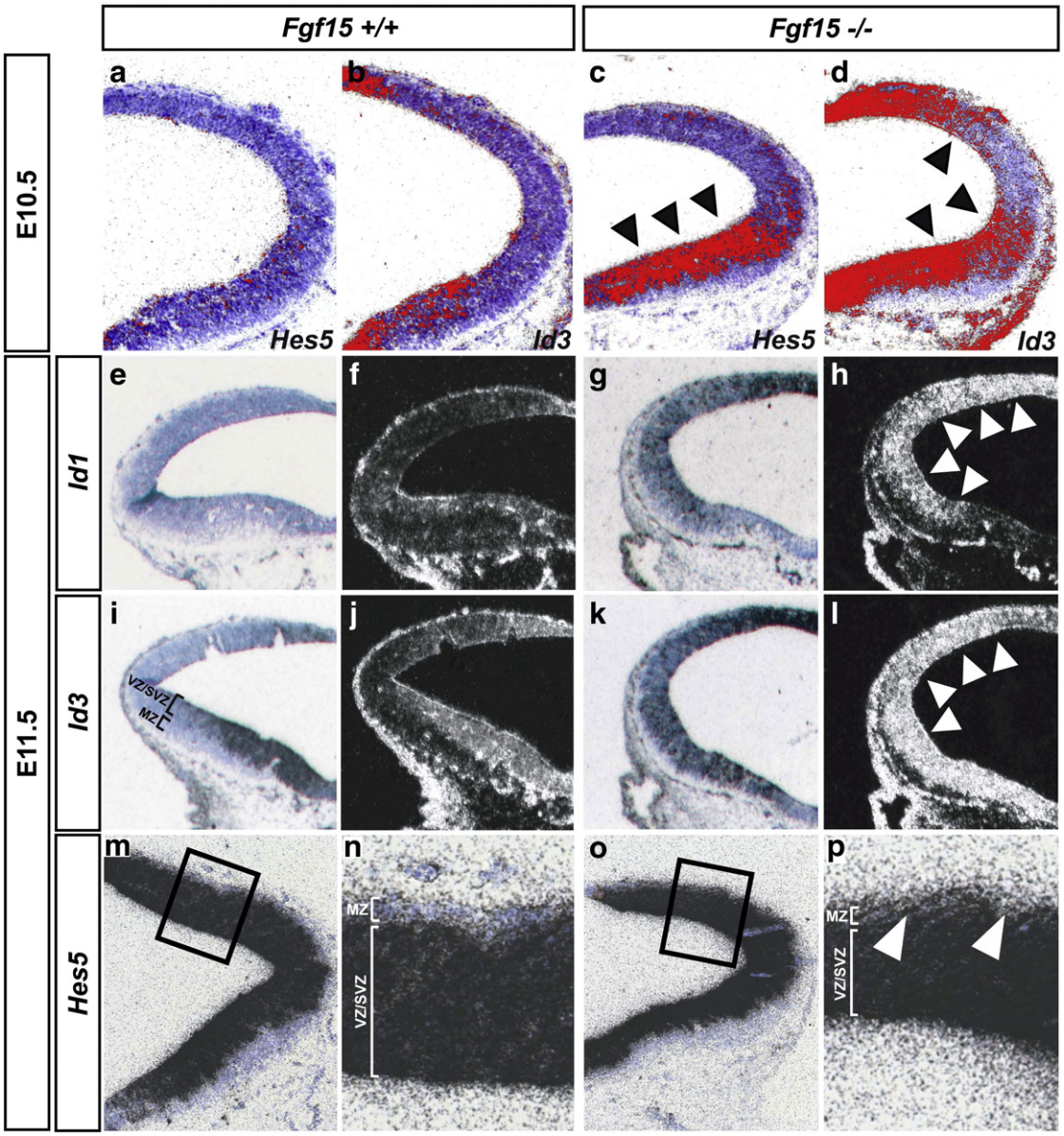

Fig. 6. Strongly increased and ectopic expression of *Id* and *Hes* genes in the *Fgf15*$^{-/-}$ dorsolateral midbrain. (a–p) Representative coronal midbrain hemisections (dorsal top) from wild-type (*Fgf15*$^{+/+}$) (a, b, e, f, i, j, m, n) and *Fgf15*$^{-/-}$ (c, d, g, h, k, l, o, p) embryos at E10.5 (a-d) and E11.5 (e–p). (f, h, j, l) are darkfield images of (e, g, i, k), respectively. (n, p) are higher magnifications of the boxed areas in (m, o). Images in (a–d) were pseudo-colored for better visualization of the ISH signal. A strong increase and ectopic expression of *Hes5* (a, c) in the ventrolateral midbrain and of *Id3* (b, d) in the dorsolateral midbrain of the *Fgf15*$^{-/-}$ embryos was already evident at E10.5 (black arrowheads in c, d). At E11.5, *Id1* (e–h) and *Id3* (i–l) expression was strongly increased and ectopically expanded (white arrowheads in h, l), whereas *Hes5* (m–p) expression extended ectopically into the MZ (white arrowheads in p) of the dorsolateral midbrain neuroepithelium in mutant embryos. Abbreviations: MZ, mantle zone; SVZ, subventricular zone; VZ, ventricular zone.

expression of proneural Ascl1, Neurog and neuronal differentiation Neurod1 HLH TFs.

Next, we analyzed the expression of two other genes involved in dorsal midbrain neurogenesis in the *Fgf15*$^{-/-}$ embryos. Transcription of the bHLH TF *Helt* (*Heslike*, *Megane*), required for the generation of dorsal midbrain GABAergic neurons (Guimera et al., 2006b; Nakatani et al., 2007), was strongly decreased in the mutant dorsolateral midbrain at E11.5 (Fig. 8). Expression of the Notch ligand *Delta-like 1* (*Dll1*), which is activated by Ascl1 and Neurog2 and promotes neuronal differentiation (Bertrand et al., 2002), was also down-regulated in the *Fgf15*$^{-/-}$ dorsolateral midbrain (Fig. 8), suggesting that dorsal midbrain neurogenesis was blocked along the proneural pathway in the absence of Fgf15.

Fgfr3 transcription is reduced in the Fgf15$^{-/-}$ *midbrain*

The intracellular signal transduction pathway activated by Fgf15 in the murine anterior neural tube is still unknown (Borello et al., 2008). We therefore analyzed the expression of Fgf signaling pathway components in the *Fgf15*$^{-/-}$ midbrain, including the Fgf receptors (*Fgfr*) *1*, *2* and *3*, the intracellular negative regulators and at the same time target genes of the mitogen-activated protein kinase (MAPK) pathway Dual specificity phosphatase 6 (*Dusp6*, *Mkp3*) and Sprouty 2 (*Spry2*), and the Fgf/MAPK target genes of the Ets family, *Etv4* (*Pea3*) and *Etv5* (*Erm*) (Mason, 2007). Expression of *Dusp6* was ectopically expanded in the mutant dorsolateral midbrain, whereas the transcription of *Fgfr3* was notably reduced in the VZ/SVZ of the *Fgf15*$^{-/-}$ midbrain including ventral domains (Fig. 8). Expression of all other genes (*Fgfr1*, *Fgfr2*, *Spry2*, *Etv4* and *Etv5*) was not altered in the mutant midbrain (Fig. 8). These results indicated that Fgf15 is required, directly or indirectly, for the regulation of *Dusp6* and *Fgfr3* transcription in the mouse midbrain.

The human ortholog FGF19 promotes cell cycle exit of mouse cortical progenitors in vitro

Based on the previous findings, we tested if recombinant human FGF19 protein, the ortholog of mouse Fgf15, promotes cell cycle exit and neuronal differentiation of cultured neural progenitor cells. We decided to use primary cortical cultures from E12.5 wild-type (CD-1) embryos for two reasons: first, because most cortical cells at this stage are neural progenitors (Borello et al., 2008), whereas dorsal midbrain neurogenesis is already peaking at E11.5–12.5 in the mouse (Edwards et al., 1986); second, because the amount and viability of neural progenitor cells that can be isolated from the mouse dorsal midbrain at E10.5–11.5 is very limited (our own observations). To follow the fate of proliferating progenitors, cultures were infected shortly after plating with a GFP-expressing retrovirus that can only integrate in replicating cells (Malatesta et al., 2000). Cell cultures were maintained in the presence of recombinant human FGF19 protein for 7 days. At day 7, we determined the number of GFP^{+} cells (cells that were proliferating at the time of retroviral infection and their progeny) and the proportion of

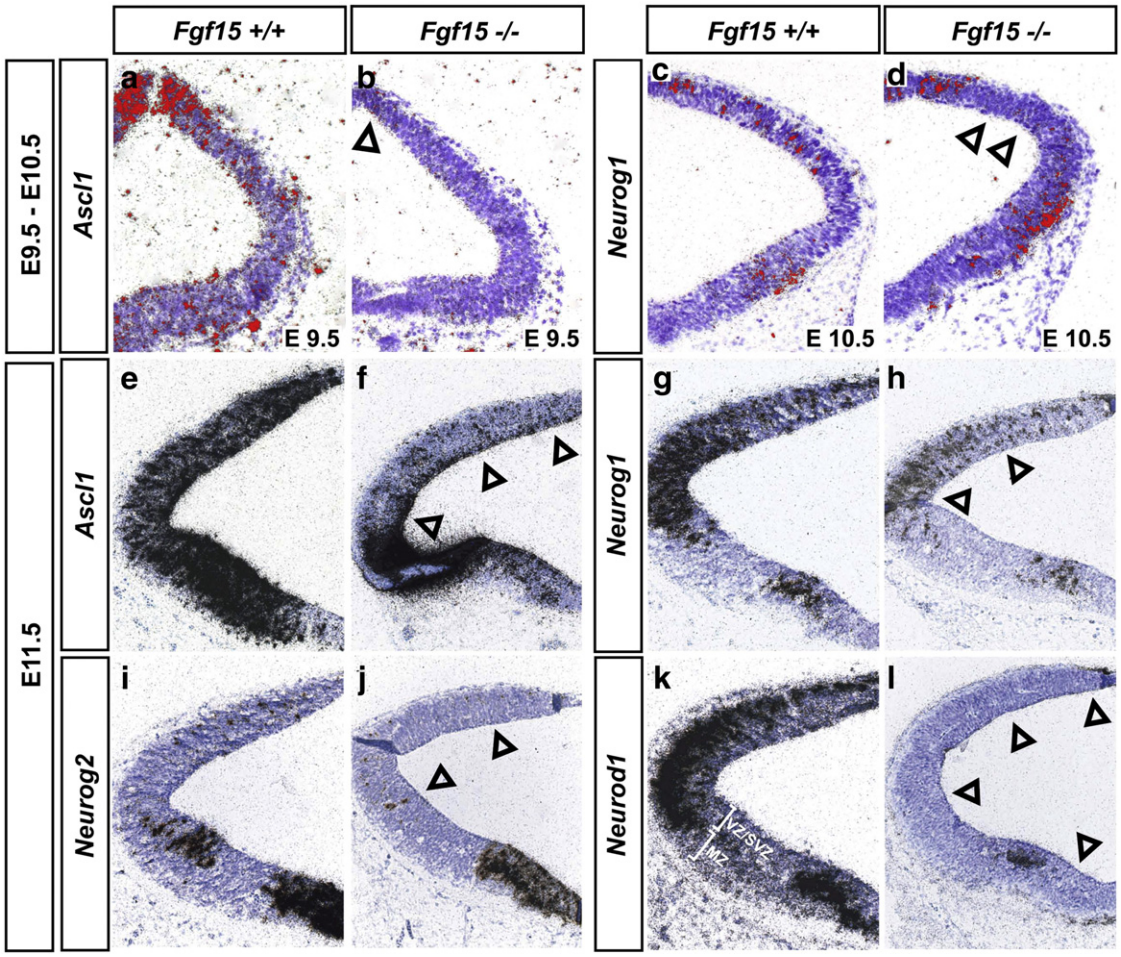

Fig. 7. Reduced or lost expression of proneural genes in the *Fgf15*$^{-/-}$ dorsolateral midbrain. (a–l) Representative coronal midbrain hemisections (dorsal top) from wild-type (*Fgf15*$^{+/+}$) (a, c, e, g, i, k) and *Fgf15*$^{-/-}$ (b, d, f, h, j, l) embryos at E9.5 (a, b), E10.5 (c, d) and E11.5 (e–l). *Ascl1* (*Mash1*; a, b, e, f) and *Neurog1* (*Ngn1*; c, d, g, h) expression was already reduced at E9.5–10.5 and strongly decreased in the mutant dorsolateral midbrain at E11.5 (open arrowheads in b, d, f, h). Transcription of *Neurog2* (*Ngn2*; i, j) was strongly decreased and of *Neurod1* (*NeuroD*; k, l) was completely abolished in the *Fgf15*$^{-/-}$ dorsolateral midbrain at E11.5 (open arrowheads in j, l). Abbreviations: MZ, mantle zone; SVZ, subventricular zone; VZ, ventricular zone.

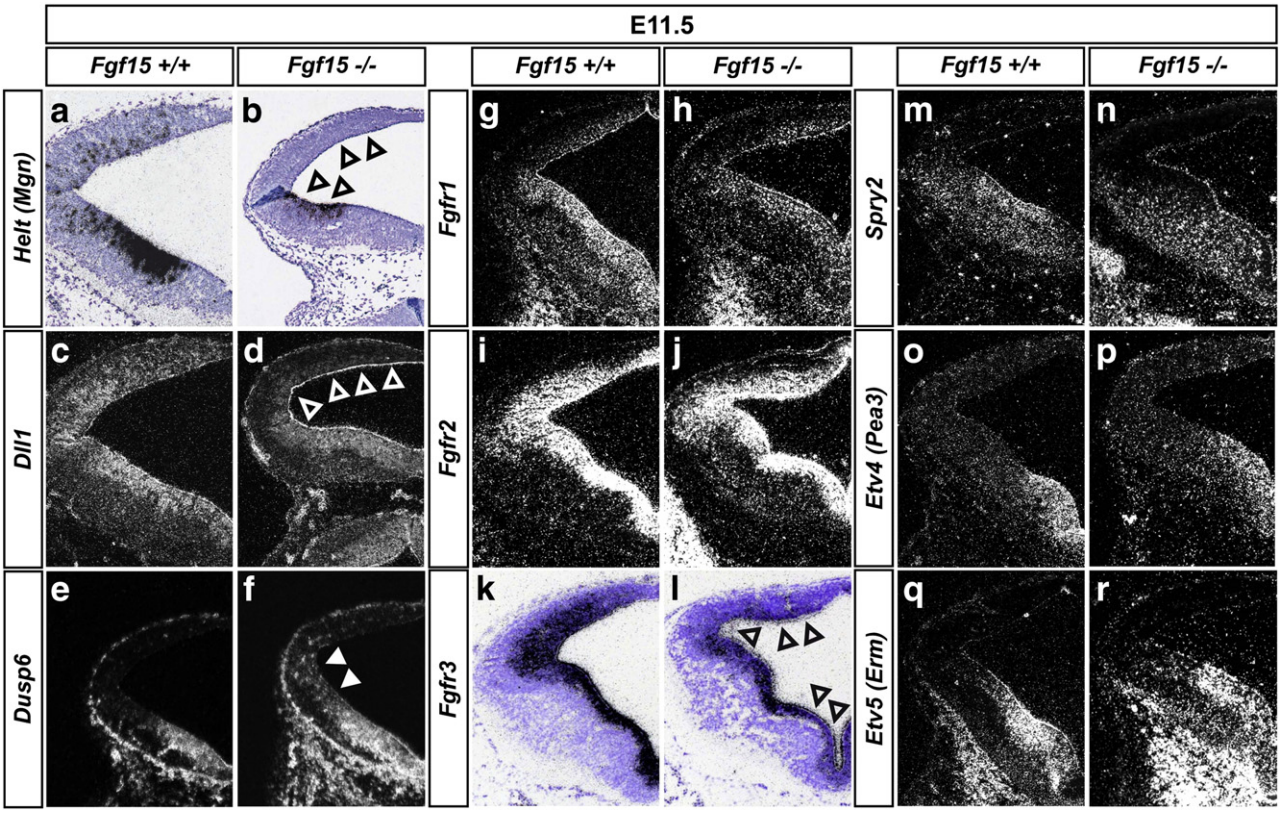

Fig. 8. Aberrant expression of other proneural genes and Fgf signal transduction components in the *Fgf15*$^{-/-}$ midbrain. (a–r) Representative coronal midbrain hemisections (dorsal top) from E11.5 wild-type (*Fgf15*$^{+/+}$) (a, c, e, g, i, k, m, o, q) and *Fgf15*$^{-/-}$ (b, d, f, h, j, l, n, p, r) embryos. (a, b, k, l) brightfield images, (c–j, m–r) darkfield images. *Helt* (*Mgn*; a, b) and *Dll1* (c, d) expression was decreased (open arrowheads in b, d), whereas *Dusp6* (*Mkp3*; e, f) transcription was increased (white arrowheads in f) in the mutant dorsolateral midbrain. *Fgfr3* (k, l) transcription was notably decreased in the entire *Fgf15*$^{-/-}$ midbrain (open arrowheads in l). Expression of *Fgfr1* (g, h), *Fgfr2* (i, j), *Spry2* (m, n), *Etv4* (*Pea3*; o, p) and *Etv5* (*Erm*; q, r) was not altered in the mutant midbrain.

these cells co-expressing Tubb3 (proliferating progenitors that had differentiated into neurons during the culture period) in the treated versus untreated cultures (Fig. 9). The total number of GFP^{+} cells was significantly reduced after FGF19 treatment, indicating that FGF19 promoted the cell cycle exit of proliferating cortical progenitors in culture (Fig. 9). Moreover, the proportion of Tubb3^{+}/GFP^{+} double-labeled cells tended to be increased in the FGF19-treated cultures, but it did not reach statistical significance (Fig. 9). We therefore concluded that treatment of mouse cortical progenitors with FGF19 significantly enhanced their cell cycle exit and tended to increase their neuronal differentiation.

Discussion

Here we show that Fgf15 controls the expression of neurogenic and proneural HLH TFs in the dorsolateral midbrain of the developing mouse embryo, thereby coordinating the postmitotic transition of dorsal neural progenitors and the initiation and progression of dorsal midbrain neurogenesis. In the absence of *Fgf15*, dorsal midbrain neural progenitors fail to exit the cell cycle and to generate the proper amount of postmitotic neurons. This defect correlates with a failure to suppress the expression of inhibitory *Id* and *Hes* HLH TFs and to activate the expression of proneural bHLH genes, leading to a massive overgrowth of dorsal neural tissues in some cases.

Fgf15 regulates the initiation and normal progression of dorsal midbrain neurogenesis by controlling the expression of neurogenic and proneural genes

Fgf15 exhibits a prominent, dynamic and graded expression in the midbrain of the midgestational mouse embryo (Gimeno et al., 2002, 2003; Ishibashi and McMahon, 2002). However, Fgf15 is not required for the regionalization of the midbrain as supported by the normal expression of early patterning genes such as *Fgf8*, *Shh*, *En1*, *Pax6*, *Wnt1* and *Wnt3a* in the *Fgf15*$^{-/-}$ embryos. This is apparently in contrast to a previous study showing that Fgf15 is required to regulate rostral patterning in the mouse forebrain (Borello et al., 2008). The reason for this discrepant role of Fgf15 in the fore- and midbrain is not known, but is most likely due to regional differences in the response to Fgf15 signaling. Moreover, the *Fgf15*$^{-/-}$ embryos displayed rather subtle changes in the expression of most cortical patterning genes analyzed by Borello et al. (2008), which could also reflect the deficits in cortical precursor proliferation and differentiation observed in these mutants, as indicated by the same authors (Borello et al., 2008).

The first evidence of an aberrant phenotype in the *Fgf15*$^{-/-}$ midbrain was detected at the beginning of the neurogenic period at around E9.5–10.5. At this time-point, the expression of certain proneural and inhibitory HLH TFs initiates in the dorsal and ventral midbrain (Andersson et al., 2006; Guillemot and Joyner, 1993; Hatakeyama and Kageyama, 2006; Kele et al., 2006). In the wild-type embryo, *Fgf15* is strongly transcribed in the dorsolateral midbrain where a few scattered *Ascl1*$^{+}$ and *Neurog1*$^{+}$ cells are first detected at E9.5–10.5, but *Fgf15* is not expressed in the mesencephalic *Id3*$^{+}$ dorsal and ventral midline (RP and FP/BP) and *Hes5* expression has not yet initiated (except for a few scattered *Hes5*$^{+}$ cells) in the midbrain at these stages (compare Fig. 1 with Figs. 6 and 7). Thus, *Fgf15* and proneural gene expression overlap in the midbrain, whereas the transcription of *Fgf15* and of inhibitory/neurogenic HLH TFs is mutually exclusive during this early neurogenic period. At later embryonic stages (E11.5–12.5), when *Fgf15* is transcribed in discrete regions with highest levels between the dorsolateral and ventrolateral sulcus of the midbrain (Fig. 1), these distinctions are less clear. At these stages, all proneural/neuronal differentiation and inhibitory/

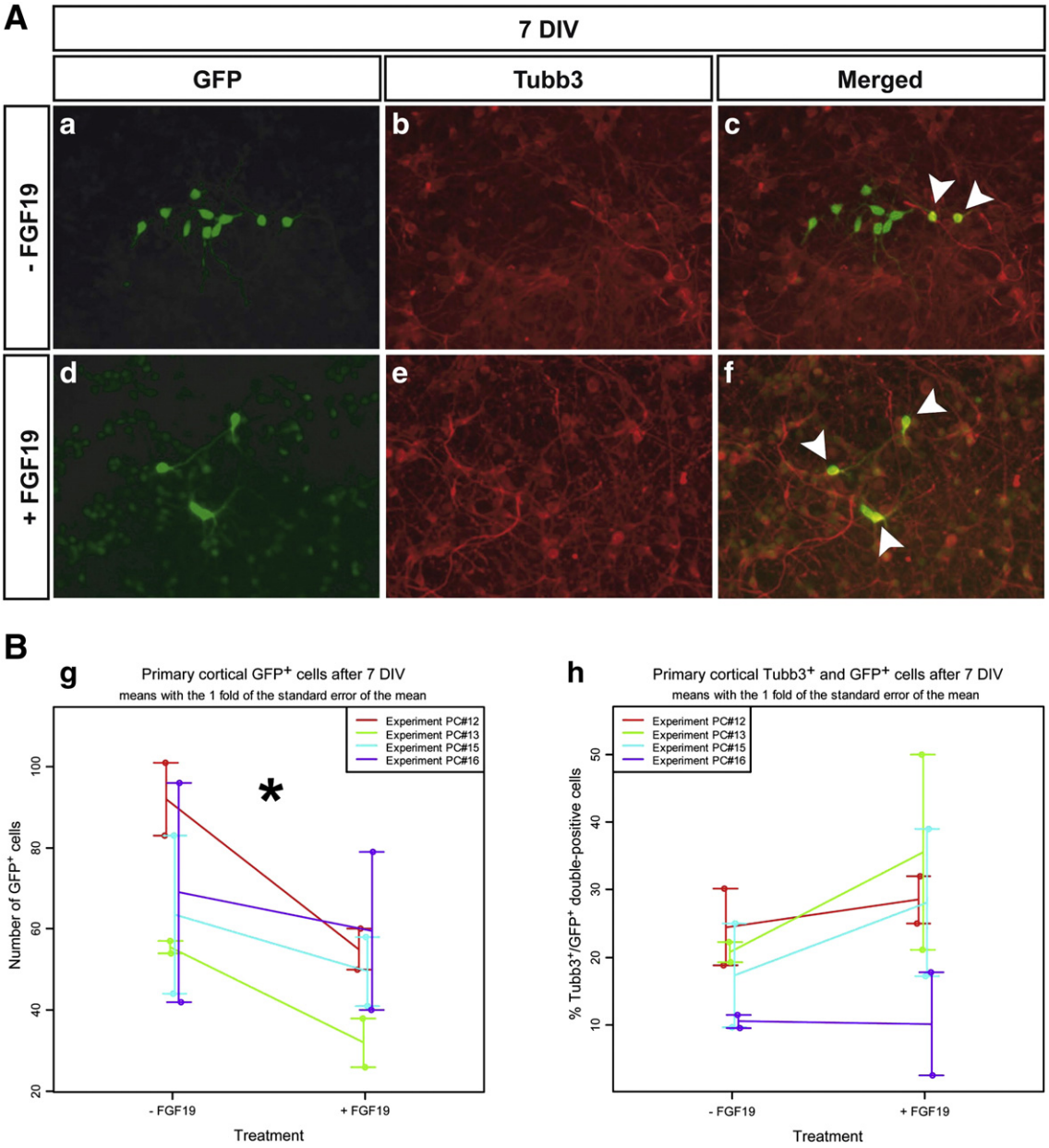

Fig. 9. The human ortholog FGF19 promotes cell cycle exit of mouse cortical progenitors in vitro. (A) Representative images of primary cortical cell cultures infected with a GFP-expressing retrovirus when plated and cultured for 7 days in vitro (DIV). Cultures were untreated (− FGF19, a–c), or maintained in the presence of recombinant human FGF19 (+ FGF19, d–f). Cells were immunostained with antibodies against GFP (green; a, d) and βIII-Tubulin (Tubb3, red; b, e); merged images are shown in (c, f). (B) Quantification of the total number of GFP^+ cells, and of $Tubb3^+/GFP^+$ double-labeled cells (white arrowheads in c, f) within each GFP^+ clone. The data shown are from four independent experiments. The total number of GFP^+ cells (proliferating progenitors at the time of retroviral infection and their progeny) was significantly reduced after FGF19 treatment (−FGF19: 70.0 ± 8.3; +FGF19: 49.0 ± 5.8, mean ± s.e.m.; two-way-ANOVA: no significant interaction ($F = 0.347$ with 3 and 8 *df*, $P = 0.79$); significant FGF19-effect in the ANOVA without interaction: $F = 5.0$ with 1 and 11 *df*, $P = 0.0464$ (asterisk)) (g). The proportion of $Tubb3^+/GFP^+$ double-labeled cells (proliferating progenitors that had differentiated into neurons during the culture period) tended to be increased after FGF19 treatment, but this increase did not reach statistical significance (−FGF19: 0.183 ± 0.027; +FGF19: 0.256 ± 0.052, mean ± s.e.m.; two-way-ANOVA: no significant interaction ($F = 0.373$ with 3 and 8 *df*, $P = 0.77$); FGF19-effect in the ANOVA without interaction: $F = 2.1$ with 1 and 11 *df*, $P = 0.176$) (h).

neurogenic genes tested are broadly expressed in the wild-type midbrain, including the *Fgf15*$^+$ domain (Figs. 6 and 7). Notably, we found that in the absence of Fgf15, the transcription of inhibitory/neurogenic *Id3* and *Hes5* genes was up-regulated and ectopically expanded, whereas that of proneural *Ascl1* and *Neurog1* genes was down-regulated in the mutant midbrain already during the early neurogenic period. The aberrant expression of inhibitory/neurogenic and proneural TFs persisted at later embryonic stages and still appeared to be most affected in the *Fgf15*$^{-/-}$dorsolateral midbrain, where *Fgf15* is highly expressed in wild-type embryos at earlier stages. This suggests that Fgf15 regulates the timing (initiation) and early phases of dorsal midbrain neurogenesis in a mostly autocrine or paracrine manner, by controlling the expression of inhibitory/neurogenic and proneural TF genes in the same or nearby cells producing Fgf15. In this context, Fgf15 might act in three ways to control the expression of these genes in the mouse midbrain (Fig. 10): 1) Fgf15 signaling might repress the transcription of inhibitory *Id3* and/or neurogenic *Hes5* HLH TFs, and thus de-repress the expression of proneural bHLH TFs (Bertrand et al., 2002; Kageyama et al., 2005); 2) Fgf15 signaling might repress only the transcription of *Id3*, which is required for the de-repression of *Hes* gene expression by inhibiting Hes binding to its own promoter (Bai et al., 2007), and thus lead to the activation of proneural bHLH TF expression; 3) Fgf15 signaling might activate the transcription of proneural *Ascl1* and/or *Neurog1* bHLH TFs, while directly or indirectly

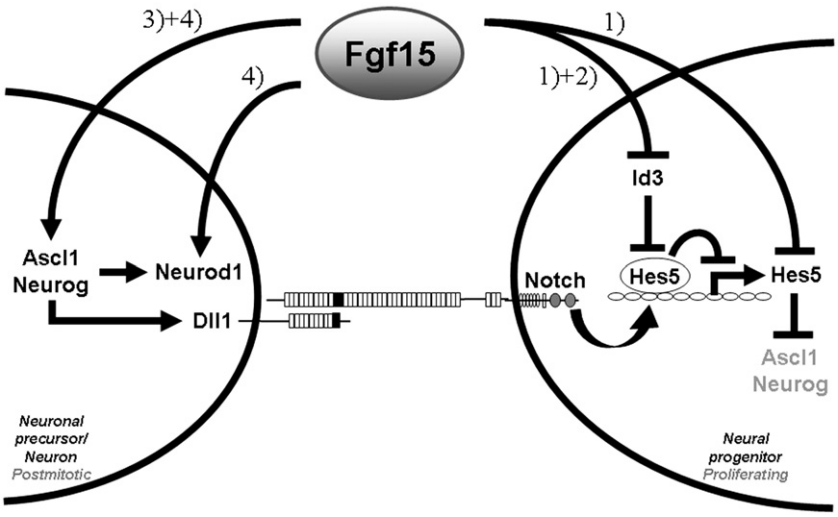

Fig. 10. Possible mechanisms of Fgf15 action in the murine dorsal midbrain. Fgf15 might promote the cell cycle exit and neuronal differentiation of neural progenitors by: 1) Repressing the expression of inhibitory Id3 and/or neurogenic Hes5 HLH TFs, thereby de-repressing the transcription of proneural bHLH TFs; 2) Repressing the expression of Id3, thereby inhibiting *Hes5* gene expression through negative autoregulation (Hes5 represses its own promoter) and de-repressing the transcription of proneural bHLH TFs; 3) Activating the transcription of proneural *Ascl1* and/or *Neurog* bHLH TFs, thereby directly or indirectly suppressing the Notch signaling pathway and *Hes* gene expression through induction of Dll1 in the same cell; 4) Activating the transcription of neuronal differentiation *Neurod1* bHLH TF directly and/or indirectly through induction of Ascl1/Neurog. See text for details. Abbreviations: Ascl1 (Mash1), Achaete–scute complex homolog 1; Dll1, Delta-like 1; Fgf15, Fibroblast growth factor 15; Hes5, Hairy and enhancer of split 5; Id3, Inhibitor of DNA binding 3; Neurod1 (NeuroD), Neurogenic differentiation 1; Neurog (Ngn), Neurogenin; Notch, Notch gene homolog.

suppressing the Notch signaling pathway and thereby expression of *Hes* genes in the same cell (Kageyama et al., 2005). In the liver, Fgf15 represses the transcription of the rate-limiting enzyme for bile acid synthesis, *Cyp7a1*, via an Fgfr4-mediated intracellular signaling pathway (Inagaki et al., 2005). It is therefore conceivable that a similar repressive mechanism might also operate in the CNS, supporting the idea of a de-repression of *Id* and *Hes* genes in the *Fgf15*$^{-/-}$ embryos.

Strikingly, the transcription of the neuronal differentiation bHLH TF *Neurod1* was completely abolished in the *Fgf15*$^{-/-}$ dorsolateral midbrain, in contrast to the residual expression of *Ascl1*, *Neurog1* and *Neurog2* in this region of the mutant brain. The loss of *Neurod1* transcription might be a direct consequence of the strongly reduced *Ascl1* and *Neurog1* expression in the *Fgf15*$^{-/-}$ embryos, as *Neurod1* is induced by these proneural TFs (Guillemot, 2007). Alternatively, Fgf15 signaling might directly control the transcription of this gene as well as of the upstream activators *Ascl1* and *Neurog*; the lack of Fgf15 signaling and strong reduction of Ascl1/Neurog expression would consequently lead to the complete abolishment of *Neurod1* transcription in the mutant dorsolateral midbrain (Fig. 10). Furthermore, proliferating neural progenitors were detected at ectopic locations within the SVZ and MZ of the *Fgf15*$^{-/-}$ dorsolateral midbrain, suggesting that some of the neural progenitors and/or precursors undergo normal migration to their neuronal target sites in the mutants. It is therefore possible that these cells enter the neuronal differentiation program but are incapable of completing it due to the lack of Neurod1. Therefore, our findings also suggest that Fgf15 regulates the proper progression of dorsal midbrain neurogenesis by controlling either directly or indirectly the expression of neuronal differentiation bHLH TF genes.

Fgf15 does not appear to control the expression of cell cycle proteins

During bone development, Fgf signaling regulates chondrocyte growth arrest and differentiation by a rapid dephosphorylation of Rb proteins and induction of cdki expression (Aikawa et al., 2001; Dailey et al., 2003; Laplantine et al., 2002). The *Fgf15*$^{-/-}$ phenotype indeed resembled the phenotype of *Rb* null mutants in certain aspects, such as embryonic lethality between E11.5 and E15.5, arrested neuronal differentiation, delayed cell cycle exit and ectopic proliferation of neural progenitors followed by massive apoptosis (Ferguson and Slack, 2001; Galderisi et al., 2003). We therefore hypothesized that Fgf15 might act via the activation/dephosphorylation of Rb and/or cdki proteins in the control of cell cycle exit and differentiation of neural progenitors. However, our data do not indicate a direct involvement of Fgf15 signaling in the regulation of cell cycle proteins such as the cdki Cdkn1b ($p27^{Kip1}$) or the Rb1/Rbl1 proteins, as the expression or phosphorylation levels of these proteins were not altered in the entire *Fgf15*$^{-/-}$ anterior neural tube.

Similarly, we did not detect an alteration in the levels of dephosphorylated (active) β-Catenin protein in the *Fgf15*$^{-/-}$ anterior neural tube (including forebrain, midbrain and rostral hindbrain), which contradicts previous findings by Borello et al. (2008) showing an increased activation of the Wnt/β-Catenin pathway in the *Fgf15*$^{-/-}$ cortex. There might be two reasons for these contradicting findings: i) Different experimental approaches were applied to determine Wnt/β-Catenin pathway activity in the *Fgf15*$^{-/-}$ embryos. Borello et al. (2008) used a Wnt/β-Catenin *LacZ* reporter (*BATgal*) allele to detect increased numbers of β-galactosidase^{+} cells in the mutants, which might be a much more sensitive approach as compared to the quantification of dephosphorylated (active) β-Catenin protein levels in brain tissue lysates by Western blot analyses used in this work. ii) Different embryonic stages were analyzed to determine Wnt/β-Catenin pathway activity in the *Fgf15*$^{-/-}$ embryos. The enhanced activation of the Wnt/β-Catenin pathway in the mutants might occur only after E11.5, which was the stage analyzed in the present work, and might thus be detected only in E12.5 and E14.5 embryos, which were the stages analyzed by Borello et al. (2008). Nevertheless, our own and previous data by Borello et al. (2008) suggest that the regulatory function of Fgf15 in the postmitotic transition of dorsal neural progenitors is conserved between the fore- and the midbrain. The proliferation of neural progenitors was increased and reduced numbers of postmitotic (Tubb3^{+}) neurons were generated in both cortex and dorsal midbrain of the *Fgf15*$^{-/-}$ embryos (Borello et al. (2008) and this work).

Complementary expression of Fg15 and Fgf8 at the MHB—functional implications

Fgf15 and *Fgf8* are expressed in a complementary pattern in the dorsal fore- and midbrain (Borello et al., 2008; Gimeno and Martinez, 2007) (this work); in particular, the dorsal mesencephalic *Fgf15*$^{+}$ region spares the *Fgf8*$^{+}$ and *Hes3*$^{+}$ (Suppl. Fig. S5) domain at the MHB. Fgf8 and Hes3 are required for the maintenance of the isthmic

organizer at the MHB, by promoting the proliferation/survival and inhibiting the premature differentiation, respectively, of the corresponding neural precursor cells (Chi et al., 2003; Hirata et al., 2001). Fgf15 has an opposite function to Hes3, by promoting the postmitotic transition and differentiation of neural precursors, and might antagonize the transcription of this gene. Consistently, the expression of *Fgf8* at the MHB was not altered (Suppl. Fig. S2), but *Hes3* expression appeared to be broadened along the rostro-caudal extent of the isthmic constriction in the *Fgf15*$^{-/-}$ embryos (Suppl. Fig. S5). This suggests that the spatial restriction of *Fgf8*/*Hes3* and *Fgf15* expression at the MHB is crucial for the proper maintenance of the isthmic organizer and consequently for the proper development of the mid-/hindbrain region, by providing a precise balance between proliferation and cell cycle exit/differentiation of neural progenitor cells within this region of the brain.

The Fgf15$^{-/-}$ *neural phenotype is only evident in an outbred genetic background*

The *Fgf15*$^{-/-}$ mice displayed a neural phenotype only when these mice were crossed into an outbred (CD-1) genetic background (this work and Borello et al. (2008)). A strong effect of genetic background was also shown for *Rbl1* (*p107*) and *Rbl2* (*p130*) null mutant mice, showing a phenotype only when backcrossed into the BALB/cJ but not in the C57BL/6 genetic background (LeCouter et al., 1998a,b). This suggests that the control of cell cycle progression and exit in neural tissues is particularly sensitive to second-site genetic modifiers having epistatic relationships with Fgf15 or Rbl1/Rbl2, respectively.

The embryonic lethality of the outbred *Fgf15*$^{-/-}$ mutants is most likely not a direct consequence of the CNS defects but rather due to the pleiotropic effects of Fgf15, including the proper formation of the cardiac outflow tract (Vincentz et al., 2005). Notably, the establishment of and blood flow in the perineural vascular plexus was not yet affected in the *Fgf15*$^{-/-}$ embryos at the stages analyzed here, indicating that the neural phenotype of the mutant embryos is not directly related to vascular or cardiac defects. The massive apoptosis of neural and non-neural tissues in around 20% of the *Fgf15*$^{-/-}$ embryos at E12.5, and the lethality of these embryos between E13.5 and E14.5, precluded the analysis of a possible later function of Fgf15 in neuronal fate determination and glial differentiation. Tissue-specific conditional mutagenesis of the *Fgf15* gene will be required to circumvent these problems.

The intracellular Fgf15 signal transduction pathway in the developing mouse CNS is still unknown but might partly differ from human and zebrafish FGF19/Fgf19

The neural phenotype of the *Fgf15*$^{-/-}$ mutants, including cell cycle irregularities and the mis-expression of neurogenic/inhibitory and proneural genes, was mostly restricted to the sites where *Fgf15* is expressed, such as the dorsolateral midbrain and forebrain (this report and Borello et al. (2008)), suggesting that Fgf15 acts locally in an autocrine or paracrine manner within the neural tube. This is in stark contrast to the known endocrine function of intestinal Fgf15 for the control of bile acid synthesis in the liver (Inagaki et al., 2005). The precise mode of action and the nature of the intracellular Fgf15 signal transduction pathway in the brain, however, remain unknown. In fact, Fgfr4 and β-Klotho, the preferential receptor and necessary co-receptor for FGF19/Fgf15 (Inagaki et al., 2005; Kurosu et al., 2007; Tomiyama et al., 2010; Xie et al., 1999), are not expressed in the developing brain at the stages analyzed here (Blak et al., 2005; Borello et al., 2008; Ito et al., 2000). We detected a notable decrease of *Fgfr3* transcription in the entire *Fgf15*$^{-/-}$ midbrain, suggesting that Fgf15 signaling directly and/or indirectly controls the expression of this Fgf receptor. A similar, selective down-regulation of *Fgfr* expression occurs in the neocortex of the *Fgf15*$^{-/-}$ embryos (Borello et al., 2008). It should be noted that *Fgfr3*$^{-/-}$ mice do not display a neural phenotype in the midbrain (Blak et al., 2007); the down-regulation of *Fgfr3* expression in the *Fgf15*$^{-/-}$ mutants is thus unlikely to be the primary cause of the *Fgf15*$^{-/-}$ midbrain phenotype. Fgfr3 acts redundantly with other Fgfr to maintain the proliferative neural progenitor pool in the dorsal telencephalon and ventral midbrain (Kang et al., 2009; Maric et al., 2007; Saarimaki-Vire et al., 2007). In this context, loss of *Fgfr* function leads to the premature depletion of neural progenitors due to their premature cell cycle exit and differentiation, which is the opposite phenotype of the *Fgf15*$^{-/-}$ mutants. The down-regulation of *Fgfr3* expression, however, might contribute additionally to the *Fgf15*$^{-/-}$ neurogenic phenotype. We also detected an up-regulation of *Dusp6* (*Mkp3*), a phosphatase that dephosphorylates Erk1/2 and thereby negatively regulates the Fgf/MAPK signaling pathway (Mason, 2007), in the *Fgf15*$^{-/-}$ dorsolateral midbrain. This suggests that Fgf15 activates the MAPK signaling pathway by repressing the expression of *Dusp6* in neural tissues. The only transient phosphorylation of Erk reported by Borello et al. (2008) after stimulation with Fgf15 of cortical progenitors in vitro, however, does not support this view.

Finally, treatment of mouse cortical progenitor cultures with recombinant human FGF19 protein increased significantly their cell cycle exit but had no significant effect on their neuronal differentiation. This discrepancy could be due to differences in the in vitro versus in vivo activity of FGF19/Fgf15, as our findings are consistent with the reduced proliferation of cortical progenitor cells after Fgf15 treatment and functional equivalence of recombinant murine Fgf15 and human FGF19 proteins in vitro reported by Borello et al. (2008). However, the failure to significantly enhance neurogenesis from FGF19-treated cortical progenitor cells might also be due to inherent mechanistic differences between Fgf15 and FGF19/Fgf19 signaling in the brain. Apart from their low homology, the developmental expression patterns of zebrafish and especially of chicken *Fgf19* differ substantially from mouse *Fgf15* (Gimeno and Martinez, 2007; Miyake et al., 2005). Moreover, zebrafish Fgf19 was reported to promote the proliferation of neural progenitors in the fore-, mid- and hindbrain of the fish (Miyake et al., 2005), in contrast to the cell cycle exit- and differentiation-inducing activity of murine Fgf15 in the fore- and midbrain of the mouse (this report and Borello et al. (2008)). Elucidation of the intracellular signaling pathway(s) and downstream targets of Fgf15 and Fgf19 in the developing vertebrate brain should help in clarifying these issues.

Acknowledgments

We would like to thank C. Murre and S.L. Mansour for providing the Fgf15$^{-/-}$ mice, M. Goetz for helpful comments and critical reading of the manuscript, A. Steiner for help with cell culture experiments, M. Costa for help with clonal analyses, O. Reiner for the Dcx antibody, S. Laass for excellent technical assistance, and Theresia Wandrowetz, Monika Nadler and Rosina Pfeiffer for animal husbandry. This work was supported by mdDANEURODEV FP7-Health-2007-B-222999 and the Italian Association for Cancer Research (AIRC) to A.S.; by Bayerischer Forschungsverbund 'ForNeuroCell II' (F2-F2412.18/10 086) and Deutsche Forschungsgemeinschaft (DFG, WU 164/4-1) to W.W. and N.P., and by the Initiative and Networking Fund in the framework of the Helmholtz Alliance of Systems Biology (CoReNe) and of Mental Health in an Ageing Society (HA-215), Federal Ministry of Education and Research (BMBF) NGFNPlus DiGtoP (FKZ 01GS0858), and European Union (mdDANEURODEV FP7-Health-2007-B-222999, EuTRACC LSHG-CT-2006-037445) to W.W.

Appendix A. Supplementary data

Supplementary data to this article can be found online at doi:10.1016/j.ydbio.2010.12.017.

References

Aikawa, T., Segre, G.V., Lee, K., 2001. Fibroblast growth factor inhibits chondrocytic growth through induction of p21 and subsequent inactivation of cyclin E-Cdk2. J. Biol. Chem. 276, 29347–29352.

Akazawa, C., Sasai, Y., Nakanishi, S., Kageyama, R., 1992. Molecular characterization of a rat negative regulator with a basic helix–loop–helix structure predominantly expressed in the developing nervous system. J. Biol. Chem. 267, 21879–21885.

Andersson, E., Tryggvason, U., Deng, Q., Friling, S., Alekseenko, Z., Robert, B., Perlmann, T., Ericson, J., 2006. Identification of intrinsic determinants of midbrain dopamine neurons. Cell 124, 393–405.

Bai, G., Sheng, N., Xie, Z., Bian, W., Yokota, Y., Benezra, R., Kageyama, R., Guillemot, F., Jing, N., 2007. Id sustains Hes1 expression to inhibit precocious neurogenesis by releasing negative autoregulation of Hes1. Dev. Cell 13, 283–297.

Benezra, R., Davis, R.L., Lockshon, D., Turner, D.L., Weintraub, H., 1990. The protein Id: a negative regulator of helix–loop–helix DNA binding proteins. Cell 61, 49–59.

Berninger, B., Costa, M.R., Koch, U., Schroeder, T., Sutor, B., Grothe, B., Gotz, M., 2007. Functional properties of neurons derived from in vitro reprogrammed postnatal astroglia. J. Neurosci. 27, 8654–8664.

Bertrand, N., Castro, D.S., Guillemot, F., 2002. Proneural genes and the specification of neural cell types. Nat. Rev. Neurosci. 3, 517–530.

Bettenhausen, B., Hrabe de Angelis, M., Simon, D., Guenet, J.L., Gossler, A., 1995. Transient and restricted expression during mouse embryogenesis of Dll1, a murine gene closely related to Drosophila Delta. Development 121, 2407–2418.

Blak, A.A., Naserke, T., Weisenhorn, D.M., Prakash, N., Partanen, J., Wurst, W., 2005. Expression of Fgf receptors 1, 2, and 3 in the developing mid- and hindbrain of the mouse. Dev. Dyn. 233, 1023–1030.

Blak, A.A., Naserke, T., Saarimaki-Vire, J., Peltopuro, P., Giraldo-Velasquez, M., Vogt Weisenhorn, D.M., Prakash, N., Sendtner, M., Partanen, J., Wurst, W., 2007. Fgfr2 and Fgfr3 are not required for patterning and maintenance of the midbrain and anterior hindbrain. Dev. Biol. 303, 231–243.

Borello, U., Cobos, I., Long, J.E., McWhirter, J.R., Murre, C., Rubenstein, J.L., 2008. FGF15 promotes neurogenesis and opposes FGF8 function during neocortical development. Neural Dev. 3, 17.

Brodski, C., Weisenhorn, D.M., Signore, M., Sillaber, I., Oesterheld, M., Broccoli, V., Acampora, D., Simeone, A., Wurst, W., 2003. Location and size of dopaminergic and serotonergic cell populations are controlled by the position of the midbrain–hindbrain organizer. J. Neurosci. 23, 4199–4207.

Cau, E., Gradwohl, G., Fode, C., Guillemot, F., 1997. Mash1 activates a cascade of bHLH regulators in olfactory neuron progenitors. Development 124, 1611–1621.

Chenn, A., Walsh, C.A., 2002. Regulation of cerebral cortical size by control of cell cycle exit in neural precursors. Science 297, 365–369.

Chi, C.L., Martinez, S., Wurst, W., Martin, G.R., 2003. The isthmic organizer signal FGF8 is required for cell survival in the prospective midbrain and cerebellum. Development 130, 2633–2644.

Choi, M., Moschetta, A., Bookout, A.L., Peng, L., Umetani, M., Holmstrom, S.R., Suino-Powell, K., Xu, H.E., Richardson, J.A., Gerard, R.D., Mangelsdorf, D.J., Kliewer, S.A., 2006. Identification of a hormonal basis for gallbladder filling. Nat. Med. 12, 1253–1255.

Christy, B.A., Sanders, L.K., Lau, L.F., Copeland, N.G., Jenkins, N.A., Nathans, D., 1991. An Id-related helix–loop–helix protein encoded by a growth factor-inducible gene. Proc. Natl Acad. Sci. USA 88, 1815–1819.

Dailey, L., Laplantine, E., Priore, R., Basilico, C., 2003. A network of transcriptional and signaling events is activated by FGF to induce chondrocyte growth arrest and differentiation. J. Cell Biol. 161, 1053–1066.

Echevarria, D., Martinez, S., Marques, S., Lucas-Teixeira, V., Belo, J.A., 2005. Mkp3 is a negative feedback modulator of Fgf8 signaling in the mammalian isthmic organizer. Dev. Biol. 277, 114–128.

Edwards, M.A., Caviness Jr., V.S., Schneider, G.E., 1986. Development of cell and fiber lamination in the mouse superior colliculus. J. Comp. Neurol. 248, 395–409.

Ferguson, K.L., Slack, R.S., 2001. The Rb pathway in neurogenesis. NeuroReport 12, A55–A62.

Fischer, T., Guimera, J., Wurst, W., Prakash, N., 2007. Distinct but redundant expression of the Frizzled Wnt receptor genes at signaling centers of the developing mouse brain. Neuroscience 147, 693–711.

Galderisi, U., Jori, F.P., Giordano, A., 2003. Cell cycle regulation and neural differentiation. Oncogene 22, 5208–5219.

Gimeno, L., Martinez, S., 2007. Expression of chick Fgf19 and mouse Fgf15 orthologs is regulated in the developing brain by Fgf8 and Shh. Dev. Dyn. 236, 2285–2297.

Gimeno, L., Hashemi, R., Brulet, P., Martinez, S., 2002. Analysis of Fgf15 expression pattern in the mouse neural tube. Brain Res. Bull. 57, 297–299.

Gimeno, L., Brulet, P., Martinez, S., 2003. Study of Fgf15 gene expression in developing mouse brain. Gene Expr. Patterns 3, 473–481.

Guillemot, F., 2007. Spatial and temporal specification of neural fates by transcription factor codes. Development 134, 3771–3780.

Guillemot, F., Joyner, A.L., 1993. Dynamic expression of the murine Achaete–Scute homologue Mash-1 in the developing nervous system. Mech. Dev. 42, 171–185.

Guimera, J., Vogt Weisenhorn, D., Echevarria, D., Martinez, S., Wurst, W., 2006a. Molecular characterization, structure and developmental expression of Megane bHLH factor. Gene 377, 65–76.

Guimera, J., Weisenhorn, D.V., Wurst, W., 2006b. Megane/Heslike is required for normal GABAergic differentiation in the mouse superior colliculus. Development 133, 3847–3857.

Hartfuss, E., Galli, R., Heins, N., Gotz, M., 2001. Characterization of CNS precursor subtypes and radial glia. Dev. Biol. 229, 15–30.

Hatakeyama, J., Kageyama, R., 2006. Notch1 expression is spatiotemporally correlated with neurogenesis and negatively regulated by Notch1-independent Hes genes in the developing nervous system. Cereb. Cortex 16 (Suppl 1), i132–i137.

Hirabayashi, Y., Itoh, Y., Tabata, H., Nakajima, K., Akiyama, T., Masuyama, N., Gotoh, Y., 2004. The Wnt/beta-catenin pathway directs neuronal differentiation of cortical neural precursor cells. Development 131, 2791–2801.

Hirata, H., Tomita, K., Bessho, Y., Kageyama, R., 2001. Hes1 and Hes3 regulate maintenance of the isthmic organizer and development of the mid/hindbrain. EMBO J. 20, 4454–4466.

Holm, S., 1979. A simple sequentially rejective multiple test procedure. Scand. J. Stat. 6, 65–70.

Inagaki, T., Choi, M., Moschetta, A., Peng, L., Cummins, C.L., McDonald, J.G., Luo, G., Jones, S.A., Goodwin, B., Richardson, J.A., Gerard, R.D., Repa, J.J., Mangelsdorf, D.J., Kliewer, S.A., 2005. Fibroblast growth factor 15 functions as an enterohepatic signal to regulate bile acid homeostasis. Cell Metab. 2, 217–225.

Ishibashi, M., McMahon, A.P., 2002. A sonic hedgehog-dependent signaling relay regulates growth of diencephalic and mesencephalic primordia in the early mouse embryo. Development 129, 4807–4819.

Ito, S., Kinoshita, S., Shiraishi, N., Nakagawa, S., Sekine, S., Fujimori, T., Nabeshima, Y.I., 2000. Molecular cloning and expression analyses of mouse betaklotho, which encodes a novel Klotho family protein. Mech. Dev. 98, 115–119.

Itoh, N., Ornitz, D.M., 2008. Functional evolutionary history of the mouse Fgf gene family. Dev. Dyn. 237, 18–27.

Jones, S., 2008. Mini-review: endocrine actions of fibroblast growth factor 19. Mol. Pharm. 5, 42–48.

Kageyama, R., Ohtsuka, T., Hatakeyama, J., Ohsawa, R., 2005. Roles of bHLH genes in neural stem cell differentiation. Exp. Cell Res. 306, 343–348.

Kageyama, R., Ohtsuka, T., Kobayashi, T., 2007. The Hes gene family: repressors and oscillators that orchestrate embryogenesis. Development 134, 1243–1251.

Kang, W., Wong, L.C., Shi, S.H., Hebert, J.M., 2009. The transition from radial glial to intermediate progenitor cell is inhibited by FGF signaling during corticogenesis. J. Neurosci. 29, 14571–14580.

Kele, J., Simplicio, N., Ferri, A.L.M., Mira, H., Guillemot, F., Arenas, E., Ang, S.-L., 2006. Neurogenin 2 is required for the development of ventral midbrain dopaminergic neurons. Development 133, 495–505.

Kurosu, H., Choi, M., Ogawa, Y., Dickson, A.S., Goetz, R., Eliseenkova, A.V., Mohammadi, M., Rosenblatt, K.P., Kliewer, S.A., Kuro-o, M., 2007. Tissue-specific expression of betaKlotho and fibroblast growth factor (FGF) receptor isoforms determines metabolic activity of FGF19 and FGF21. J. Biol. Chem. 282, 26687–26695.

Kuwabara, T., Hsieh, J., Muotri, A., Yeo, G., Warashina, M., Lie, D.C., Moore, L., Nakashima, K., Asashima, M., Gage, F.H., 2009. Wnt-mediated activation of NeuroD1 and retro-elements during adult neurogenesis. Nat. Neurosci. 12, 1097–1105.

Laplantine, E., Rossi, F., Sahni, M., Basilico, C., Cobrinik, D., 2002. FGF signaling targets the pRb-related p107 and p130 proteins to induce chondrocyte growth arrest. J. Cell Biol. 158, 741–750.

LeCouter, J.E., Kablar, B., Hardy, W.R., Ying, C., Megeney, L.A., May, L.L., Rudnicki, M.A., 1998a. Strain-dependent myeloid hyperplasia, growth deficiency, and accelerated cell cycle in mice lacking the Rb-related p107 gene. Mol. Cell. Biol. 18, 7455–7465.

LeCouter, J.E., Kablar, B., Whyte, P.F., Ying, C., Rudnicki, M.A., 1998b. Strain-dependent embryonic lethality in mice lacking the retinoblastoma-related p130 gene. Development 125, 4669–4679.

Lendahl, U., Zimmerman, L.B., McKay, R.D., 1990. CNS stem cells express a new class of intermediate filament protein. Cell 60, 585–595.

Ma, Q., Sommer, L., Cserjesi, P., Anderson, D.J., 1997. Mash1 and neurogenin1 expression patterns define complementary domains of neuroepithelium in the developing CNS and are correlated with regions expressing notch ligands. J. Neurosci. 17, 3644–3652.

Malatesta, P., Hartfuss, E., Gotz, M., 2000. Isolation of radial glial cells by fluorescent-activated cell sorting reveals a neuronal lineage. Development 127, 5253–5263.

Maric, D., Fiorio Pla, A., Chang, Y.H., Barker, J.L., 2007. Self-renewing and differentiating properties of cortical neural stem cells are selectively regulated by basic fibroblast growth factor (FGF) signaling via specific FGF receptors. J. Neurosci. 27, 1836–1852.

Mason, I., 2007. Initiation to end point: the multiple roles of fibroblast growth factors in neural development. Nat. Rev. Neurosci. 8, 583–596.

McWhirter, J.R., Goulding, M., Weiner, J.A., Chun, J., Murre, C., 1997. A novel fibroblast growth factor gene expressed in the developing nervous system is a downstream target of the chimeric homeodomain oncoprotein E2A-Pbx1. Development 124, 3221–3232.

Megason, S.G., McMahon, A.P., 2002. A mitogen gradient of dorsal midline Wnts organizes growth in the CNS. Development 129, 2087–2098.

Minowada, G., Jarvis, L.A., Chi, C.L., Neubuser, A., Sun, X., Hacohen, N., Krasnow, M.A., Martin, G.R., 1999. Vertebrate Sprouty genes are induced by FGF signaling and can cause chondrodysplasia when overexpressed. Development 126, 4465–4475.

Miyake, A., Nakayama, Y., Konishi, M., Itoh, N., 2005. Fgf19 regulated by Hh signaling is required for zebrafish forebrain development. Dev. Biol. 288, 259–275.

Nakatani, T., Minaki, Y., Kumai, M., Ono, Y., 2007. Helt determines GABAergic over glutamatergic neuronal fate by repressing Ngn genes in the developing mesencephalon. Development 134, 2783–2793.

Nguyen, L., Besson, A., Roberts, J.M., Guillemot, F., 2006. Coupling cell cycle exit, neuronal differentiation and migration in cortical neurogenesis. Cell Cycle 5, 2314–2318.

Nishimura, T., Utsunomiya, Y., Hoshikawa, M., Ohuchi, H., Itoh, N., 1999. Structure and expression of a novel human FGF, FGF-19, expressed in the fetal brain. Biochim. Biophys. Acta 1444, 148–151.

Parr, B.A., Shea, M.J., Vassileva, G., McMahon, A.P., 1993. Mouse Wnt genes exhibit discrete domains of expression in the early embryonic CNS and limb buds. Development 119, 247–261.

Pinheiro, J., Bates, D., DebRoy, S., Sarkar, D., R Development Core Team, 2008. nlme: Linear and Nonlinear Mixed Effects Models 2008.

Puelles, E., Acampora, D., Lacroix, E., Signore, M., Annino, A., Tuorto, F., Filosa, S., Corte, G., Wurst, W., Ang, S.L., Simeone, A., 2003. Otx dose-dependent integrated control of antero-posterior and dorso-ventral patterning of midbrain. Nat. Neurosci. 6, 453–460.

Puelles, E., Annino, A., Tuorto, F., Usiello, A., Acampora, D., Czerny, T., Brodski, C., Ang, S.L., Wurst, W., Simeone, A., 2004. Otx2 regulates the extent, identity and fate of neuronal progenitor domains in the ventral midbrain. Development 131, 2037–2048.

R Development Core Team, 2009. R: A language and environment for statistical computing. Vienna, Austria: R Foundation for Statistical Computing. http://www.R-project.org.

Roussa, E., Wiehle, M., Dunker, N., Becker-Katins, S., Oehlke, O., Krieglstein, K., 2006. Transforming growth factor beta is required for differentiation of mouse mesencephalic progenitors into dopaminergic neurons in vitro and in vivo: ectopic induction in dorsal mesencephalon. Stem Cells 24, 2120–2129.

Ruzinova, M.B., Benezra, R., 2003. Id proteins in development, cell cycle and cancer. Trends Cell Biol. 13, 410–418.

Saarimaki-Vire, J., Peltopuro, P., Lahti, L., Naserke, T., Blak, A.A., Vogt Weisenhorn, D.M., Yu, K., Ornitz, D.M., Wurst, W., Partanen, J., 2007. Fibroblast growth factor receptors cooperate to regulate neural progenitor properties in the developing midbrain and hindbrain. J. Neurosci. 27, 8581–8592.

Siegenthaler, J.A., Miller, M.W., 2005. Transforming growth factor beta 1 promotes cell cycle exit through the cyclin-dependent kinase inhibitor p21 in the developing cerebral cortex. J. Neurosci. 25, 8627–8636.

Theiler, K., 1989. The House Mouse. Atlas of embryonic development. Springer Verlag, New York.

Tomiyama, K., Maeda, R., Urakawa, I., Yamazaki, Y., Tanaka, T., Ito, S., Nabeshima, Y., Tomita, T., Odori, S., Hosoda, K., Nakao, K., Imura, A., 2010. Relevant use of Klotho in FGF19 subfamily signaling system in vivo. Proc. Natl Acad. Sci. USA 107, 1666–1671.

Vincentz, J.W., McWhirter, J.R., Murre, C., Baldini, A., Furuta, Y., 2005. Fgf15 is required for proper morphogenesis of the mouse cardiac outflow tract. Genesis 41, 192–201.

Wexler, E.M., Paucer, A., Kornblum, H.I., Plamer, T.D., Geschwind, D.H., 2009. Endogenous Wnt signaling maintains neural progenitor cell potency. Stem Cells 27, 1130–1141.

Wright, T.J., Ladher, R., McWhirter, J., Murre, C., Schoenwolf, G.C., Mansour, S.L., 2004. Mouse FGF15 is the ortholog of human and chick FGF19, but is not uniquely required for otic induction. Dev. Biol. 269, 264–275.

Xie, M.H., Holcomb, I., Deuel, B., Dowd, P., Huang, A., Vagts, A., Foster, J., Liang, J., Brush, J., Gu, Q., Hillan, K., Goddard, A., Gurney, A.L., 1999. FGF-19, a novel fibroblast growth factor with unique specificity for FGFR4. Cytokine 11, 729–735.